AN ANALYSIS OF WIRE DRAWING UNDER HYDRODYNAMIC LUBRICATION

A Thesis Submitted
in Partial Fulfilment of the Requirements
for the Degree of

MASTER OF TECHNOLOGY

by

DINESHCHANDRA N. DAVE

to the

DEPARTMENT OF MECHANICAL ENGINEERING
INDIAN INSTITUTE OF TECHNOLOGY KANPUR

JUNE, 1982

ME-1982-M-DAN-ANA.

CERTIFICATE

This is to certify that the work entitled 'AN ANALYSIS OF WIRE DRAWING UNDER HYDRODYNAMIC LUBRICATION' by Mr. D.N. Dave has been carried out under my supervision and has not been submitted elsewhere for a degree.

(G.K. LAL)
Professor,
Department of Mechanical Engineering,
Indian Institute of Technology,
KANPUR - 208016.

ACKNOWLEDGEMENTS

I wish to express my gratitude to Dr. G.K. Lal for his helpful guidance and constant encouragement at all stages of work.

My thanks are due to Messers V. Raghuram, M.K. Vohra, A.K. Srivastava and Y.J. Shah for the co-operation extended for the experimental work.

I express my thanks to Messers B.P. Bhartia, R.M. Jha and Joginder Singh for their help whenever needed.

Thanks are also due to Mr. J.P. Gupta for neat typing.

DINESH N. DAVE

CONTENTS

NOMENCLATURE

A	:	Area of cross-section of the wire
A'	:	Constant of integration, equation (36)
a	:	Constant, equation (71-a)
B	:	Material constant, equation (73)
b	:	Constant, equation (71-b)
C	:	Constant, equation (32)
C_1, C_2	:	Constants, equation (7-a)
C_3	:	Constant, equation (55-b)
C_4	:	Constant, equation (58)
D	:	Diameter of wire
$\bar{e}$	:	Generalised plastic strain
f	:	Redundant work factor
h	:	Lubricant film thickness
K	:	Constant, equation (52)
m	:	Material constant, equation (73)
P	:	Pressure of the lubricant
Q	:	Volume flow rate of lubricant
R	:	Drawing ratio (A_1/A_2)
S	:	Sommerfeld number
S_c	:	Critical Sommerfeld number
u	:	Axial velocity of the wire
V	:	Velocity of the lubricant along the wire surface

Greek Symbols:

α : Semi die angle

η : Dynamic viscosity of lubricant

σ : Axial stress in the wire

$\bar{\sigma}$: Generalised plastic stress

$\bar{\sigma}_o$: Generalised yield stress for rigid, perfectly plastic material

σ_o : Generalised yield stress of wire material before drawing

τ : Shear stress

Subscripts:

1 : Entry point

2 : Exit point

Z : Any point in the deformation zone

ABSTRACT

Most of the analyses of wire drawing operation have been carried out assuming dry friction in the interface zone. A few hydrodynamic lubrication models have also been presented and are based on the principle of minimum rate of entropy production and have used assumed variation of film thickness in the interface zone.

In the present analysis an attempt has been made to present a hydrodynamic model of wire drawing so as to predict the variation of film thickness in the interface zone. The lubricant viscosity has also been assumed to be pressure dependent. The thickness of the oil film has been obtained using equilibrium equations in the deformation zone and the generalised Reynolds equation for lubricant flow. The criterion for sustained hydrodynamic lubrication has been evaluated in terms of critical Sommerfeld number.

Analytical results obtained by idealising the wire material to be rigid, perfectly plastic shows good agreement with the experimental values of drawing and separating forces.

The effect of redundant work is also included in this analysis. The solution in this case is obtained in close form. The analysis has then been extended to include the effect of strain hardening and the results shows very close agreement with the experimentally measured values. The solution,

however, requires the use of numerical technique.

The analysis indicates that the true hydrodynamic lubrication can be obtained at very high drawing speed which are not likely to be realised in practice. In most cases therefore only quasi hydrodynamic lubrication is likely to be achieved. Experiments indicates that ringing wear in the die is absent even when only quasi hydrodynamic lubrication is achieved.

CHAPTER - I

INTRODUCTION

1.1 Introduction

During the process of wire drawing, the principal function is to make a wire of a specified size. This is done by pulling the wire through a die with a tapered bore, as shown in Fig. 1.1. Wire deforms plastically within the confines of the die due to triaxial stress system produced as a result of the pull and nip of the die.

Severe die wear occurs when the wire is drawn at high speeds. Typical die life for tungsten carbide and diamond dies being 80-325 Km and 1.6 - 13×10^{6} Km per 2.54×10^{-2} mm increase of die bore, respectively. In such situations lubricants play a very important role. The functions of lubricant in wire drawing are quite complex in comparison to other applications. In wire drawing, lubricants are used to minimize friction and temperature in order to prolong the die life. It also protects the wire from rusting and imparts lustre to the drawn wire.

During wire drawing for surface finish, the role of lubricant film is essentially to prevent scuffing of wire and die; but the lubricant film should be thin so as not to interfere with the burnishing action at the die-wire interface. Ideally, best method for this purpose seems to be dry friction or boundary lubrication. When the function of drawing is merely

to reduce the size of the wire, a thick film lubrication can be advantageous, since it provides low friction and large heat capacity and the job may be done in the least number of passes, at a higher speed with reduced die wear and power. In such situations hydrodynamic lubrication is definitely advantageous.

1.2 Hydrodynamic Lubrication

The function of a lubricant is to separate the sliding surfaces by a thin film, thus reducing the metal to metal contact. This phenomenon, based on the film thickness, can be classified as a boundary layer lubrication and hydrodynamic lubrication.

The boundary layer lubrication is said to prevail when a lubricant film thickness is only one or two molecular layer thick and it takes place under high normal pressure and at a low sliding speed. In this type of lubrication, the friction is influenced by the nature of the underlying metal surfaces and the chemical nature of the lubricant and not by the bulk properties of the lubricant such as a density and viscosity.

Hydrodynamic lubrication prevails when a lubricant film is of appreciable thickness so as to completely separate the sliding surfaces. Viscosity and other bulk properties of the lubricant governs the resistance to the sliding motion.

Christopherson and Naylor [1] observed that the amount of lubricant passing through the die is often much greater than

that corresponding to a layer of molecular thickness. The thickness of the oil film as observed from the measured flow was about 10^{-3} mm. Appreciable electrical resistance across the die-wire interface during drawing with soap or wax as lubricant has also been measured [2], from which it was concluded that even at moderate drawing speeds the lubricant film could be 3×10^{-3} mm thick. Evidence was also presented which indicated that the film was thicker for small die angles and light reductions during drawing of soft wires.

These effects seems to indicate the existence of hydrodynamic lubrication condition in wire drawing. The phenomenon of wire drawing in the presence of hydrodynamic lubrication at die-wire interface has not been thoroughly investigated. The principle of minimum rate of entropy production was employed in theoretical studies of hydrostatic extrusion [3] and cold strip rolling [4], under hydrodynamic lubrication conditions, to evaluate the film thickness.

Bedi [5] employed the principle of minimum rate of entropy production, together with the equilibrium equations, to evaluate the film thickness and viscous friction coefficient during wire drawing with hydrodynamic lubrication. He assumed a variation of film thickness, in the deformation zone, to be (i) constant and (ii) exponential in his studies.

Avitzur [6] obtained the upper bound on power for rolling with hydrodynamic lubrication. He expressed the

relative exit velocity and relative thickness of the lubricant film as a function of independant process variables.

An experimental and theoretical study of the process of drawing wire through a device based on adaptation of Christopherson tube and employing a polymer melt as the lubricanting agent, was studied by Hashmi et al. [7]. In this study, an empirical expression relating shear stress and rate of shear, together with an experimentally derived pressure coefficient of viscosity, was utilized for determining the coating thickness possible on the wire. Coating thickness was observed to be of the order of 5×10^{-2} mm.

Drupad Ram [8] studied the hydrodynamic lubrication in wire drawing considering strain hardening, strain rate, temperature and redundant work. He also assumed a linear variation of film thickness in his theoretical analysis.

1.3 Present Work

A review of the literature indicates that the very few attempts have been made to analyse the metal forming operations taking into account the effects of lubrication. A few hydrodynamic lubrication models have been presented. These are based on the principal of minimum rate of entropy production and have used assumed variation in the film thickness at the interface zone.

In the present work an attempt have been made to present a hydrodynamic model of wire drawing so as to predict the variation in the film thickness in the interface zone. The lubricant viscosity has also been assumed to be pressure dependent. The film thickness has been obtained by using the equilibrium equation in the deformation zone and the generalised Reynolds equation for the lubricant flow for hydrodynamic lubrication. The drawing stress and the pressure at the interface have been obtained for both rigid perfectly plastic, and strain hardening materials. The effects of redundant work have been included in the analysis. The hydrodynamic lubrication conditions have been evaluated in terms of critical Sommerfeld number and the results obtained have been compared with experiments.

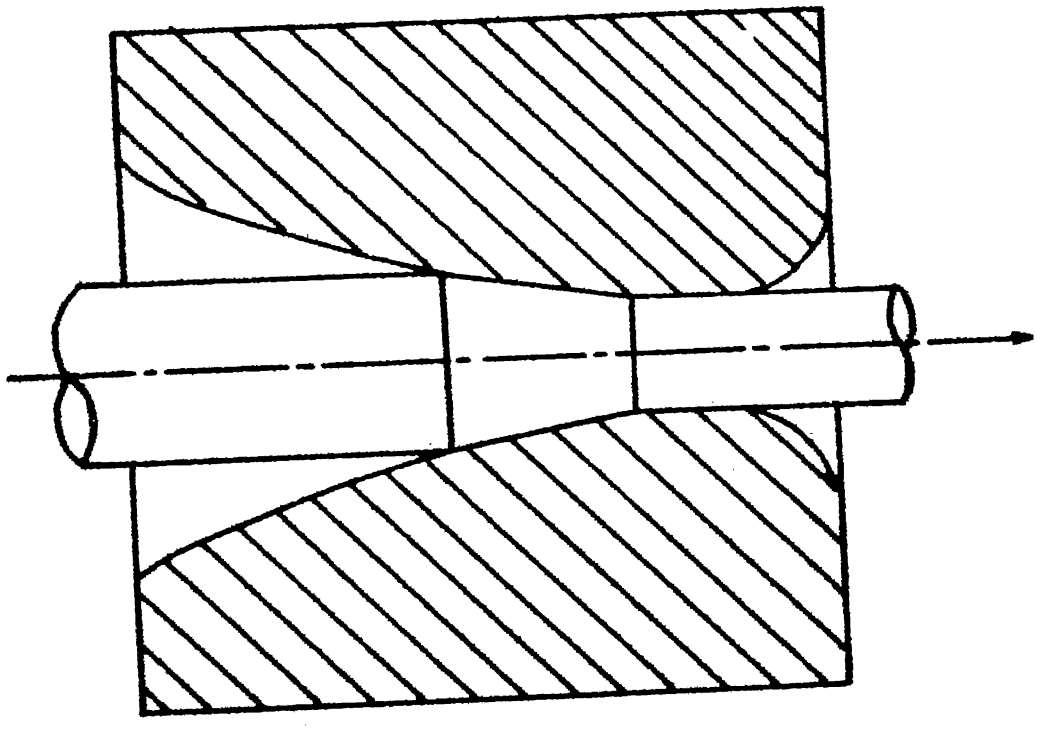

Fig. 1.1 Wire drawing die

CHAPTER - II

HYDRODYNAMIC MODEL

2.1 Introduction

Hydrodynamic lubrication prevails in wire drawing when the lubricant film prevents the wire from contacting the die. Hydrodynamic lubrication is normally effected by the fast moving wire, dragging the liquid lubricant into the interface zone.

Under hydrodynamic lubrication conditions, the characteristics of friction become a function of the interface geometry, lubricant viscosity and speed. If the viscosity can be characterized and measured, the understanding of frictional behaviour during hydrodynamic lubrication is better understood then when metal-to-metal contact prevails.

The studies of hydrodynamic lubrication in some metal forming processes use two or more pseudo-independent parameters which are dictated by the principle of minimum energy or least resistance. These parameters are considered as being determined by the independent variables which, in turn, are dictated by the process geometry, machine set-up and prescribed boundary conditions.

In the present analysis equilibrium equation in the deformation zone has been used along with the generalized Reynolds equation to study the hydrodynamic lubrication aspects in wire drawing.

2.2 Basic Assumptions

(a) For Wire Material :

(1) The material to be drawn is an incompressible homogeneous and isotropic material obeying von Mises yield criterion and associated flow rule.

(2) Elastic strains are negligible compared to plastic strains.

(3) The plastic flow of the material in the deformation zone is a isothermal flow.

(b) For Lubricant :

(1) The lubricant is a Newtonian fluid and its flow is laminar.

(2) Lubricant fluid is incompressible.

(3) The lubricant flow occurs under isothermal condition.

(c) Additional Assumptions :

(1) During deformation of the wire material, a plane section of the wire remains plane and the deformation of a plane element is homogeneous.

(2) The lubricant film is assumed to extend over the whole of the interface between die and wire and the film thickness is small compared to the diameter of the wire.

2.3 Analysis

2.3.1 Equilibrium Equation

Referring to Fig. 2.1 and equating stresses in the axial direction gives

$$-\sigma_Z \frac{\pi D^2}{4} + (\sigma_Z + d\sigma_Z) \frac{\pi}{4} (D+dD)^2 + P(\pi D dx) \sin\alpha + \tau(\pi D dx) \cos\alpha = 0 \qquad (1)$$

Where, σ_Z is the longitudinal stress in the wire, D is the wire diameter in the conical portion of the die (variable), p is the normal pressure on the wire in the die, α is the half die angle, τ is the shear stress acting on the wire at the die-wire interface.

Rearranging and neglecting higher powers of dD gives

$$D d\sigma_Z + 2\sigma_Z dD + 4P\sin\alpha\, dx + 4\tau\cos\alpha\, dx = 0$$

Also,

$$\sin\alpha = D/2x \quad \text{and} \quad dD = 2\sin\alpha\, dx \qquad (2)$$

Hence

$$x d\sigma_Z + 2\sigma_Z dx + 2P dx + 2\tau\cot\alpha\, dx = 0$$

or

$$x d\sigma_Z + 2dx(\sigma_Z + P + \tau\cot\alpha) = 0.$$

The Von-Mises yield criterion [1] gives

$$\sigma_Z + P = \bar{\sigma} \qquad (3)$$

where, $\bar{\sigma}$ is a generalized yield stress.

Hence,

$$x \frac{d\sigma_Z}{dx} + 2\bar{\sigma} + \frac{2\tau}{\tan\alpha} = 0$$

or

$$x\left(\frac{dP}{dx} - \frac{d\bar{\sigma}}{dx}\right) - 2\bar{\sigma} - \frac{2\tau}{\tan\alpha} = 0 \qquad (4)$$

2.3.2 Film Thickness

For a fully developed Newtonian laminar flow of the lubricant between the die and the wire material, and assuming the taper of the lubricant wedge to be shallow, the Reynold's equation [9] is

$$\frac{dP}{dx} = \eta \frac{d^2V}{dy^2} \qquad (5)$$

where, η is the viscosity and V is the velocity of the lubricant.

Double integration yields

$$V = \frac{y^2}{2\eta}\frac{dP}{dx} + C_1 y + C_2 \qquad (6)$$

The following boundary conditions

$$y = 0 \; ; \quad V = 0$$

$$y = h \; ; \quad V = -u_1 \quad \text{in the inlet zone}$$

$$V = -u_1\left(\frac{x_1}{x}\right)^2 \quad \text{in the deformation zone}$$

$$V = -u_2 = -u_1\left(\frac{x_1}{x}\right)^2 \quad \text{in the outlet region.} \qquad (7)$$

yield

$$C_2 = 0 \quad \text{and} \quad C_1 = -\frac{u_1}{h}\left(\frac{x_1}{x}\right)^2 - \frac{1}{2\eta}\frac{dP}{dx}\,h \qquad (7\text{-a})$$

Hence,

$$V = \frac{1}{2\eta}\frac{dP}{dx}\,(y^2 - yh) - \frac{u_1}{h}\,y \quad \text{in the inlet zone} \qquad (8)$$

$$V = \frac{1}{2\eta}\frac{dP}{dx}\,(y^2 - yh) - \frac{u_1}{h}\left(\frac{x_1}{x}\right)^2 y \quad \text{in the deformation zone.} \qquad (9)$$

The rate of lubricant flow, Q, is given by

$$Q = \pi D \int_0^h V \, dy \qquad (10)$$

Using equations (2) and (9), equation (10) yields

$$\frac{Q}{2\pi \sin\alpha} = -x \left[\frac{h^3}{12\eta} \frac{dP}{dx} + \frac{u_1}{2} \left(\frac{x_1}{x}\right)^2 h \right] \qquad (11)$$

From the geometry of the film thickness

$$h = x\tan\alpha - D/2\cos\alpha \qquad (12)$$

From equation (11)

$$\frac{dP}{dx} = -\frac{12\eta}{h^3} \left[\frac{Q}{2\pi x \sin\alpha} + \frac{u_1}{2} \left(\frac{x_1}{x}\right)^2 h \right] \qquad (13)$$

The shear stress, τ, on the wire surface due to viscous shearing of the lubricant [9] is

$$\tau = -\eta \left(\frac{dV}{dy} \right)_h \qquad (14)$$

Substituting for V from equation (9) gives

$$\left(\frac{dV}{dy} \right)_h = \frac{1}{2\eta} \frac{dP}{dx} h - \frac{u_1}{h} \left(\frac{x_1}{x} \right)^2 \qquad (15)$$

Substituting for $\left(\frac{dV}{dy}\right)_h$ in equation (14) gives

$$\tau = \frac{\eta u_1}{h} \left(\frac{x_1}{x}\right)^2 - \frac{h}{2} \frac{dP}{dx} \qquad (16)$$

Assuming the wire material to be rigid perfectly plastic, that is

$$\bar{\sigma} = \bar{\sigma}_o = \text{constant} \tag{17}$$

or

$$\frac{d\bar{\sigma}}{dx} = 0 \tag{18}$$

Equation (4), therefore, reduces to

$$x \frac{dP}{dx} - 2\bar{\sigma}_o - \frac{2\tau}{\tan\alpha} = 0 \tag{19}$$

Substituting for τ from equation (16) gives

$$x \frac{dP}{dx} - 2\bar{\sigma}_o - \frac{2\eta u_1}{h \tan x} \left(\frac{x_1}{x}\right)^2 = 0 \tag{20}$$

Since he is very small.

Hence, in the inlet zone at $x = x_1$

$$\left.\frac{dP}{dx}\right|_{x_1} = \frac{2}{x_1} \left[\bar{\sigma}_o + \frac{\eta u_1}{h_1 \tan\alpha} \right] \tag{21}$$

From equation (11), in the inlet zone

$$Q = - \left[\frac{h^3}{12\eta} \frac{dP}{dx}_{x_1} + \frac{u_1 h_1}{2} \right] 2\pi x_1 \sin\alpha \tag{22}$$

Substituting for $\left.\frac{dP}{dx}\right|_{x_1}$ from equation (21) gives

$$Q = -\left[\frac{h_1^3}{12\eta}\frac{2}{x_1}\left(\bar{\sigma}_o + \frac{\eta u_1}{h_1 \tan\alpha}\right) + \frac{u_1 h_1}{2}\right] 2\pi x_1 \sin\alpha \quad (23)$$

Hence, for the deformation zone, equation (13) gives

$$\frac{dP}{dx} = \frac{12\eta}{h^3}\left[\frac{h_1^3}{6\eta x}\left(\bar{\sigma}_o + \frac{\eta u_1}{h_1 \tan\alpha}\right) + \frac{u_1 x_1}{2x}\left(h_1 - \frac{x_1}{x} h\right)\right] \quad (24)$$

Equation (20) also gives $\frac{dP}{dx}$ for the deformation zone as

$$\frac{dP}{dx} = \frac{2}{x}\left[\bar{\sigma}_o + \frac{\eta u_1}{h \tan\alpha}\left(\frac{x_1}{x}\right)^2\right] \quad (25)$$

Equating equations (24) and (25) gives

$$\frac{h_1^3}{6\eta x}\left(\bar{\sigma}_o + \frac{\eta u_1}{h_1 \tan\alpha}\right) + \frac{u_1 x_1}{2x}\left(h_1 - \frac{x_1}{x} h\right) = \frac{h^3}{6\eta x}\left[\bar{\sigma}_o + \frac{\eta u_1}{h \tan x}\left(\frac{x_1}{x}\right)^2\right] \quad (26)$$

Neglecting higher order terms of h, equation (26) reduces to

$$\frac{u_1 x_1}{2x}\left(h_1 - \frac{x_1}{x} h\right) = 0 \quad (27)$$

This yields,

$$h = h_1 \frac{x}{x_1} \tag{28}$$

Equation (28) shows that the variation of film thickness in the deformation zone is linear.

2.3.3 Film Thickness at the Entry side of Die

The rate of lubricant flow, Q, in the entry zone can also be evaluated using equations (8) and (10) as

$$Q = -\pi D \left[\frac{h^3}{12\eta} \frac{dP}{dx} + \frac{u_1 h}{2} \right] \tag{29}$$

Therefore

$$\frac{dP}{dx} = -\eta u_1 \left[\frac{12Q}{\pi D u_1 h^3} + \frac{6}{h^2} \right] \tag{30}$$

or

$$\frac{dP}{dx} = -\eta u_1 \left(\frac{C+6h}{h^3} \right), \tag{31}$$

where

$$\frac{12Q}{\pi D u_1} = C = \text{Constant.} \tag{32}$$

The viscosity of liquid exhibits a greater pressure variation, the pressure-effect correlation being of the type [1]

$$\eta = \eta_o e^{\nu P} , \qquad (33)$$

where η_o is the dynamic viscosity of lubricant at atmospheric pressure and ν is the pressure coefficient of viscosity of lubricant.

Increase in the temperature also takes place due to irreversible plastic deformation of the wire material within the deformation zone. If the residence time of the metal in the deformation zone is sufficiently small, of the order of few microseconds, the heat convected to the lubricant will be negligible. The temperature dependence of the viscosity can, therefore, be neglected.

Equations (31) and (33) gives

$$\frac{dP}{dx} = - \eta_o e^{\nu P} u_1 \left(\frac{C + 6x \tan\alpha}{x^3 \tan^3\alpha} \right) \qquad (34)$$

Since $h = x\tan\alpha$ in this region.

Integration of equation (34) gives

$$- \frac{e^{-\nu P}}{\nu} = \frac{\eta_o u_1 C}{\tan^3\alpha} \cdot \frac{1}{2x^2} + \frac{6 \eta_o u_1}{x \tan^2\alpha} + A' \qquad (35)$$

The constant A' in this equation can be evaluated from the consideration that $P = 0$ at $x = x_o$, i.e. at point O (Fig.2.2).

On substituting this condition, equation (35) gives

$$A' = -\left[\frac{1}{\nu} + \frac{\eta_o u_1}{\tan^2\alpha}\left(\frac{6}{x_o} + \frac{C}{2\tan\alpha - x_o^2}\right)\right] \qquad (36)$$

and equation (35) becomes

$$-\frac{e^{-\nu P}}{\nu} = \frac{\eta_o u_1 C}{2\tan^3\alpha \cdot x^2} + \frac{6\eta_o u_1}{x\tan^2\alpha} - \frac{1}{\nu} - \frac{\eta_o u_1}{\tan^2\alpha}\left(\frac{6}{x_o} + \frac{C}{2x_o^2\tan\alpha}\right) \qquad (37)$$

Assuming the yielding to take place at $x = x_n$, where $h = h_n$, and neglecting $e^{-\nu P}$, since this is small compared to other terms because of higher pressure, equation (37) reduces to

$$\frac{\eta_o u_1 C}{2x_1^2\tan^3\alpha} + \frac{6\eta_o u_1}{x_1\tan^2\alpha} - \frac{1}{\nu} - \frac{\eta_o u_1}{\tan^2\alpha}\left(\frac{6}{x_o} + \frac{C}{2x_o^2\tan\alpha}\right) = 0 \qquad (38)$$

On rearranging terms in this equation,

$$C = \frac{2h_o^2 h_n^2 \tan\alpha}{\eta_o u_1 \nu (h_o^2 - h_n^2)} - \frac{12 h_1 h_n}{h_1 + h_n} \qquad (39)$$

Since,

$$x_o = h_o/\tan\alpha \quad \text{and} \quad x_n = h_n/\tan\alpha. \qquad (40)$$

The rate of lubricant flow in the inlet region, from equation (32), is

$$Q = \frac{\pi D u_1 C}{12} \tag{41}$$

Q in this region can also be evaluated from equation (11), which gives

$$Q = -\pi D \left[\frac{h^3}{12\eta} \frac{dP}{dx} + \frac{u_1}{2} \left(\frac{x_1}{x} \right)^2 h \right]$$

Neglecting higher order terms of h in the above equation, Q at entry point, where $x = x_1$, is obtained as

$$Q = -\frac{\pi D u_1 h_n}{2} \tag{42}$$

Equating equations (41) and (42), we have

$$Q = \frac{\pi D_1 u_1 C}{12} = -\frac{\pi D u_1 h_n}{2}$$

or

$$C = -6 h_n \tag{43}$$

Substituting for C in equation (39) gives

$$-6 h_n = \frac{2 h_o^2 h_n^2 \tan\alpha}{\eta_o u_1 (h_o^2 - h_n^2)} - \frac{12 h_n h_o}{h_n + h_o}$$

Rearranging the terms in the above equation yields

$$6h_n^2 + 6h_o^2 - 12\, h_n h_o - A h_n h_o = 0, \qquad (44)$$

where

$$A = \frac{2h_o \tan\alpha}{\eta_o u_1 \sqrt{}} \qquad (45)$$

Solution of this quadratic equation in h_n is

$$h_n = h_o \left[1 + \frac{A}{12}\left\{1 - \sqrt{1 + \frac{24}{A}}\right\}\right]$$

$$= h_o \left[1 + \frac{A}{12}\left\{1 - \left(1 + \frac{12}{A} - \frac{1}{8}\left(\frac{24}{A}\right)^2 ---\right)\right\}\right]$$

$$\approx \frac{6\, h_o}{A} \qquad (46)$$

Substituting for A from equation (45) into above equation yields

$$h_n \approx \frac{3\, \eta_o u_1 \sqrt{}}{\tan\alpha} = h_1. \qquad (47)$$

Equation (47) gives the approximate value of the lubricant film thickness at the entry point in the die, i.e, at $x = x_1$ (Fig.2.1). Knowing the film thickness at entry point, film thickness at any point in the deformation zone can be obtained using equation (28).

2.3.4 Alternative method of evaluating Film Thickness at the entry side

Equation (20) can be written as

$$\frac{x}{2}\frac{dP}{dx} = \bar{\sigma}_o + \frac{\eta u_1}{h_1 \tan\alpha}\left(\frac{x_1}{x}\right)^3 \qquad (48)$$

Let $\frac{x}{x_1} = Z$ then $dZ = \frac{dx}{x_1}$ and equation (48) becomes

$$\frac{dP}{dZ} = \frac{2\bar{\sigma}_o}{Z} + \frac{2\eta u_1}{h_1 \tan\alpha} \cdot \frac{1}{Z^4}$$

Also

$$\eta = \eta_o e^{\nu P}$$

Therefore

$$e^{-\nu P}\frac{dP}{dZ} = \frac{2\bar{\sigma}_o}{Z} e^{-\nu P} + \frac{2\eta_o u_1}{h_1 Z^4 \tan\alpha} \qquad (49)$$

Solution of the above differential equation gives

$$e^{-\nu P} = \frac{2\eta_o u_1 \nu}{h_1 \tan\alpha\,(2\nu\bar{\sigma}_o - 3)} \cdot \frac{1}{Z^3} + \frac{K}{Z^{2\nu\bar{\sigma}_o}}, \qquad (50)$$

where K is the constant of integration.

Using the boundary condition

$$x = x_1 \; ; \quad Z = 1 \; ; \quad P_1 = \bar{\sigma}_o - \sigma_1 \; , \tag{51}$$

where σ_1 is the back tension applied on the wire. Equation (50) now yields

$$K = \bar{e}^{\nu(\bar{\sigma}_o - \sigma_1)} + \frac{2\eta_o u_1 \nu}{h_1 \tan\alpha \, (2\nu\bar{\sigma}_o - 3)} \tag{52}$$

and equation (50) becomes

$$\bar{e}^{\nu P} = - \frac{2\eta_o u_1 \nu}{h_1 \tan\alpha (2\nu\bar{\sigma}_o - 3)} \cdot \frac{1}{Z^3} + \frac{\bar{e}^{\nu(\bar{\sigma}_o - \sigma_1)}}{Z^{2\nu\bar{\sigma}_o}}$$

$$+ \frac{2\eta_o u_1 \nu}{h_1 \tan\alpha \, (2\nu\bar{\sigma}_o - 3)} \cdot \frac{1}{Z^{2\nu\bar{\sigma}_o}} \tag{53}$$

Using equation (24), we have

$$\frac{dP}{dx}\bigg|_{x_1} = - \frac{12\eta}{h^3} \left[- \frac{h_1^3}{12\eta} \cdot \frac{2}{x_1} \left(\bar{\sigma} + \frac{\eta u_1}{h_1 \tan\alpha} \right) - \frac{u_1 h_1}{2} + \frac{u_1}{2} h \left(\frac{x_1}{x} \right)^2 \right]$$

(54)

or

$$\frac{dP}{dx}_{x_1} = \frac{12\,\eta_o e^{\gamma P}}{h^3}\left(C_3 - \frac{u_1 h}{2}\right), \qquad (55\text{-a})$$

where

$$C_3 = -\frac{h_1^3}{6\,\eta x_1}\left(\bar{\sigma} + \frac{\eta_o u_1 e^{\gamma P_1}}{h_1 \tan\alpha}\right) - \frac{u_1 h_1}{2} \qquad (55\text{-b})$$

Also

$$h = x\tan\alpha - \frac{D}{2}\cos\alpha.$$

Since $dD = 0$ at $x = x_1$, $dh = dx\tan\alpha$.

Equation (55) can, therefore, be rewritten as

$$\tan\alpha\,\frac{dP}{dh} = \frac{12\,\eta_o e^{\gamma P}}{h^3}\left(C_3 - \frac{u_1 h}{2}\right) \qquad (56)$$

Integration of this equation yields

$$-\frac{e^{-\gamma P}}{\gamma} = \frac{12\,\eta_o}{\tan\alpha}\left(-\frac{C_3}{2h^2} + \frac{u_1}{2h}\right) + C_4 \qquad (57)$$

Further, as $h \to \infty$, $p \to 0$ at the wire surface. This condition gives

$$C_4 = -\frac{1}{\gamma} \qquad (58)$$

and equation (57) becomes

$$\frac{1}{\nu}\left(1-\bar{e}^{\nu P}\right) = \frac{12\,\eta_o}{\tan\alpha}\left(-\frac{C_3}{2h^2}+\frac{u_1}{2h}\right) \qquad (59)$$

Now at $x = x_1$,

$$P = \bar{\sigma}_o - \sigma_1 \quad \text{and} \quad h = h_1.$$

Substituting these conditions in equation (59) and neglecting h_1 in comparison to $1/h_1$ gives

$$1-\bar{e}^{\nu P_1} \simeq \frac{3\,\eta_o \nu\, u_1}{h_1 \tan\alpha} - \frac{\eta_o u_1 \nu}{x_1 \tan^2\alpha} \qquad (60)$$

or

$$h_1 = \frac{3\,\eta_o \nu\, u_1}{\tan\alpha} \cdot \frac{1}{\left(1-\bar{e}^{\nu P_1} + \frac{\eta_o u_1 \nu}{x_1 \tan^2\alpha}\right)} \qquad (61)$$

Equation (47), for h_1, was derived assuming $\bar{e}^{\nu P}$ to be negligible compared to other terms in the equation (35). Equation (61) gives more exact value of film thickness at the entry point. This equation will also reduce to equation (47) when viscosity of lubricant is low and $\bar{e}^{\nu P_1}$ is of negligible value, i.e. when yield stress is high and back tension is very small.

2.3.5 Drawing stress

Now, at $x = x_2$,

$$Z = \frac{x_2}{x_1} = \frac{1}{\sqrt{R}} \quad \text{and} \quad P = P_2 = \bar{\sigma}_o - \sigma_2$$

where

$R = A_1/A_2$, the drawing ratio

Hence, equation (53) may be rewritten as

$$e^{-\nu(\bar{\sigma}_o-\sigma_2)} = \frac{2\eta_o u_1 \nu}{h_1 \tan\alpha\,(2\nu\bar{\sigma}_o-3)} \cdot (R^{\nu\bar{\sigma}_o} - R^{3/2}) + e^{-\nu(\bar{\sigma}_o-\sigma_1)} \cdot R^{\nu\bar{\sigma}_o} \tag{62}$$

The above equation gives the relationship between the drawing stress, drawing ratio and back tension.

Substituting for h_1 from equation (61) into equation (62) gives

$$e^{-\nu(\bar{\sigma}_o-\sigma_2)} = \frac{2}{3}\left(1-e^{-\nu P_1} + \frac{\eta_o u_1 \nu}{x_1 \tan^2\alpha}\right) \cdot \left(\frac{R^{\nu\bar{\sigma}_o} - R^{3/2}}{2\nu\bar{\sigma}_o-3}\right) + e^{-\nu(\bar{\sigma}_o-\sigma_1)} \cdot R^{\nu\bar{\sigma}_o} \tag{63}$$

or

$$e^{\nu(\sigma_2-\sigma_1)} = R^{\nu\bar{\sigma}_o}\left[1+\frac{2}{3}\left(\frac{(\frac{3}{2}-\nu\bar{\sigma}_o)}{2\nu\bar{\sigma}_o-3}\right)\left(-1+e^{\nu(\bar{\sigma}_o-\sigma_1)} + \frac{u_1\eta_o\nu\, e^{\nu(\bar{\sigma}_o-\sigma_1)}}{x_1 \tan^2\alpha}\right)\right] \tag{64}$$

Taking logarithm on both sides and rearranging terms the above equation becomes

$$\sigma_2-\sigma_1 = \bar{\sigma}_o \ln R + \frac{1}{\gamma} \ln\left[1+ \frac{2}{3}\left(\frac{1-R^{\left(\frac{3}{2}-\gamma\bar{\sigma}_o\right)}}{2\gamma\bar{\sigma}_o - 3}\right)\left\{-1+e^{\gamma(\bar{\sigma}_o-\sigma_1)} + \frac{u_1\eta_o\gamma\, e^{\gamma(\bar{\sigma}_o - \sigma_1)}}{x_1 \tan^2\alpha}\right\}\right] \qquad (65)$$

This equation gives the relationship between the drawing stress, drawing ratio, speed of drawing, back tension, viscosity of lubricant, yield stress and initial diameter of wire and half die angle. The first term on right hand side of this equation represents homogeneous work of deformation and the second term indicates the contribution of frictional work. The term on the left hand side can be identified as the contribution of external work needed for drawing under hydrodynamic lubrication.

A non-dimensional term S can be defined as,

$$S = \frac{u_1\eta_o\gamma}{x_1\tan^2\alpha} \cdot e^{\gamma(\bar{\sigma}_o-\sigma_1)} \qquad (66)$$

S is of the same form as the Sommerfeld number used in the theory of hydrodynamic bearing [9].

Since,

$$\sin\alpha = D_1/2\,x_1$$

and for small value of α, $\tan\alpha = \sin\alpha$, therefore,

$$D_1 \approx 2\,x_1 \tan\alpha$$

Hence,

$$S = \frac{2\,u_1\eta_o\nu\, e^{\nu(\bar{\sigma}_o-\sigma_1)}}{D_1 \tan\alpha} \qquad (67)$$

Equation (61) can now be rewritten in terms of S as,

$$h_1 = \frac{3}{2} S D_1 \frac{1}{(S - 1 + e^{\nu(\bar{\sigma}_o-\sigma_1)})} \qquad (68)$$

Assuming that the die is perfectly smooth, the initial film thickness h_1 should be greater than the surface roughness h_o of the wire for sustained hydrodynamic lubrication, i.e.,

$$\frac{3}{2} S D_1 \frac{1}{(S - 1 + e^{\nu(\bar{\sigma}_o-\sigma_1)})} \geq h_o \qquad (69)$$

A critical condition will prevail when $h_1=h_o$ and let $S=S_c$ at that instant. Then at the critical condition,

$$\frac{3}{2} S_c D_1 \cdot \frac{1}{(S - 1 + e^{\gamma(\bar{\sigma}_o - \sigma_1)})} = h_o$$

or

$$\frac{S_c}{S_c - 1 + e^{\gamma(\bar{\sigma}_o - \sigma_1)}} = \frac{2}{3} \frac{h_o}{D_1}$$

or

$$S_c = \frac{b(e^a - 1)}{1 - b}, \qquad (70)$$

where,

$$a = (\bar{\sigma}_o - \sigma_1) \qquad (71\text{-a})$$

and

$$b = \frac{2}{3} \frac{h_o}{D_1}. \qquad (71\text{-b})$$

Similarly equation (65) can also be rewritten in term of S as

$$\sigma_2 = \sigma_1 + \bar{\sigma}_o \ln R + \frac{1}{\gamma} \ln \left[1 + \frac{2}{3}\left(\frac{1-R}{2\gamma\bar{\sigma}_o - 3}\right)\left\{-1 + e^{\gamma(\bar{\sigma}_o - \sigma_1)} + S_c\right\}\right] \qquad (72)$$

2.3.6 Strain Hardening Effect

During the plastic deformation the metal strain hardens and the nature of the strain-stress curve depends on the

material. Strain hardening effect, neglecting the temperature and the strain rate effects, can be included in the analysis by using an equation of the form [10],

$$\bar{\sigma} = \sigma_o + B(\bar{e})^m , \tag{73}$$

where $\bar{\sigma}_o$, B and m are material constants.

Effect of redundant work due to shearing can be included by replacing $\bar{e}$ with $\bar{e}^* = f \cdot \bar{e}$ in equation (73), where f is the redundant work factor. The value of f for a range of metals and lubricants is quoted by Rowe [11]. Thus,

$$f = 0.87 + \left(\frac{1}{R-1} \right) \sin\alpha \tag{74}$$

For the process under consideration,

$$\bar{e} = \ln \left(\frac{A_1}{A} \right) = 2 \ln \left(\frac{x_1}{x} \right) \tag{75}$$

The equilibrium equation (4) can now be rewritten as

$$x\left(\frac{dP}{dx} - \frac{d}{dx}(\sigma_o + B(\bar{e})^m)\right) - 2(\sigma_o + B(\bar{e})^m) - \frac{2\eta_o \dot{e} P u_1}{h \tan\alpha} \left(\frac{x_1}{x}\right)^2 = 0 \tag{76}$$

Since,

$$h = \frac{x}{x_1} h_1 \quad \text{and} \quad \bar{e} = 2 \ln\left(\frac{x_1}{x} \right)$$

The above equation can be written as

$$x\frac{dP}{dx} + (2f)^m B\, m\, ln^{m-1}\left(\frac{x_1}{x}\right) - 2\sigma_o - 2B(2f)^m ln^m\left(\frac{x_1}{x}\right) - \frac{2\eta_o u_1 e^{\nu P}}{h_1 \tan\alpha}\left(\frac{x_1}{x}\right)^3 = 0 \qquad (77)$$

or

$$\frac{dP}{dx} = \left\{2\sigma_o + 2^{m+1}\cdot B\cdot f^m\cdot ln^m\left(\frac{x_1}{x}\right) + \frac{2\eta_o u_1 e^{P}}{h_1 \tan\alpha}\left(\frac{x_1}{x}\right)^3 - (2f)^m\cdot B\cdot m\cdot ln^{m-1}\left(\frac{x_1}{x}\right)\right\}\cdot\frac{1}{x} \qquad (78)$$

The solution of the above equation can be obtained using Euler's numerical method which gives

$$P_{i+1} = P_i + \Delta x_{i+1}\left(\frac{dP}{dx}\right)_i \qquad (79)$$

where

$$\Delta x_{i+1} = x_{i+1} - x_i$$

Hence, using equation (78) through (79)

$$P_{i+1} = P_i + \frac{\Delta x_{i+1}}{x_i}\left\{2\sigma_o + (2f)^m 2B\, ln^m\left(\frac{x_1}{x_i}\right) + \frac{2\eta_o u_1 e^{\nu P_i}}{h_1 \tan\alpha}\left(\frac{x_1}{x_i}\right)^3 - (2f)^m B\, m\, ln^{m-1}\left(\frac{x_1}{x_i}\right)\right\} \qquad (80)$$

The boundary condition is

$$x = x_1 \quad ; \quad P_1 = \sigma_o - \sigma_1$$

Since P is known at the starting point, P_2, P_3, P_4, etc. can be evaluated using equation (80).

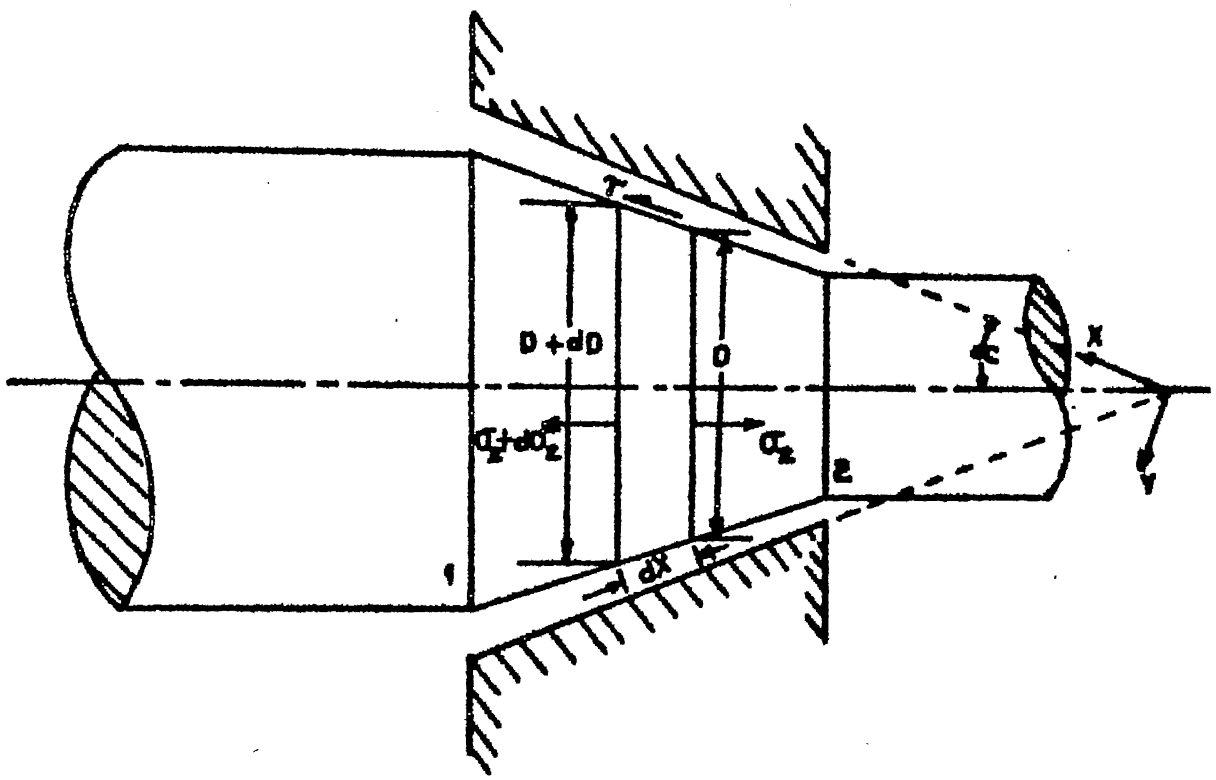

Fig. 2.1 Stresses on element of wire material

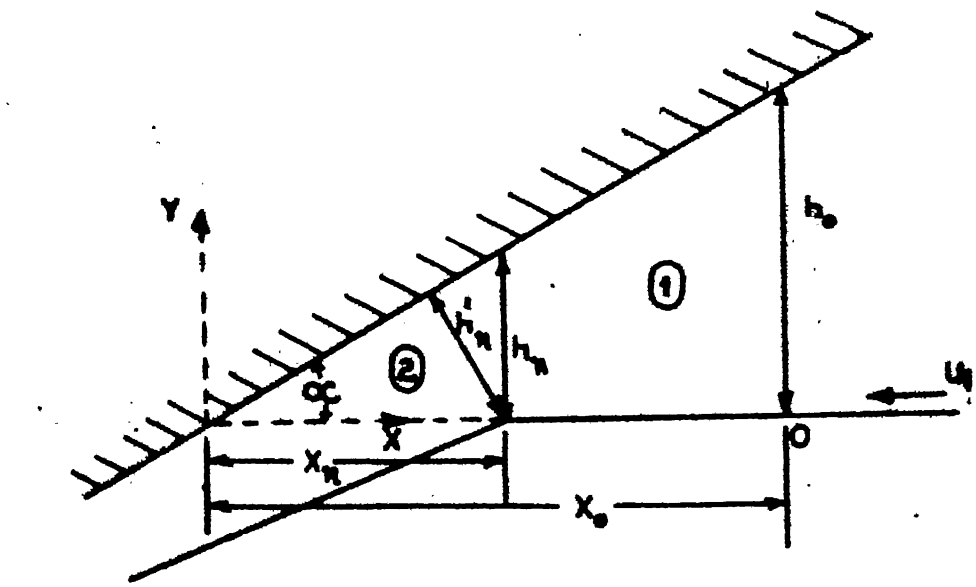

Fig. 2.2 Die-wire interface zone

CHAPTER - III

EXPERIMENTS

3.1 Wire Drawing Set-up

A single-block, single-die, single-pass, vertical Wire Drawing Machine of 300 mm diameter drum was used for experimental purposes. The machine was fitted with a gear box to provide drawing speeds in the range of 12.93 to 77.79 m/min in five steps. The specifications of the machine are given in Appendix-I.

3.2 Lubricant Feed Device

The lubricant feed device on the machine was modified in line with the Christopherson's experimental set-up [1] where the wire is made to approach the die through a tube of diameter slightly larger than the wire diameter and sealed onto the inlet side of the die. This arrangement was capable of generating pressure comparable with the yield stress of the wire at the entry side of the die. This helps in achieving true hydrodynamic lubrication. The die, mounted on the dynamometer plate, was held tight against the Christopherson tube and the lubricant chamber was attached to the forward end of the Christopherson tube. The tube used was 2.3 mm diameter and 80 mm long. The complete set-up is shown in Fig. 3.1.

3.3 Dynamometer

The dynamometer used for measuring the drawing and separating forces is shown diagramatically in Fig. 3.2. It consists of an elastic circular disc which is supported at its periphery. A 20 mm tapered bore made in the central boss at a taper angle of 12 degrees holds the split die in position. Semiconductor strain gauges attached at AA'BB' measure the drawing force, while strain gauges CC'DD' measure the separating forces (Fig. 3.2). Dummy gauges EE'FF' are used to complete the bridge circuit for separating force measurement. The circuit diagrams for measurement of forces are shown in Fig. 3.3. The dynamometer output signals were fed to a two channel Encardio-Rite pen recorder for continuous recording of forces.

The dynamometer was calibrated by pushing a tapered plug through the tapered split die held in the tapered boss. The output from the two bridge circuits were recorded simultaneously. The calibration set-up on a lathe is shown in Fig.3.4. The calibration curves are shown in Fig. 3.5. The details regarding evaluation of drawing and separating forces are given in Appendix-II.

3.4 Split Die

Specially made HSS split dies, dies made in two halves, were used for the experiments. Using this type of dies it is

possible to measure both the drawing and separating forces simultaneously using the above mentioned dynamometer. Detail specifications of dies are given in Appendix-III.

3.5 Wire Material

Mild steel wire of 2.08 mm diameter was used for the experiments. All experiments were conducted using wire from a single roll. Stress-Strain curve for the wire material (Fig. 3.6) was obtained on an Instron machine. Curve fitting gave the following stress-strain relation for the wire material :

$$\bar{\sigma} = 260 + 246.2\,(\bar{e})^{0.63} \quad N/mm^2$$

3.6 Lubricant

A light machine oil of viscosity 65 centipoise at $28^{\circ}C$ and atmospheric pressure was used as the lubricant. The viscosity of the lubricant was experimentally evaluated using Brookfield Viscometer. The pressure dependence of the viscosity was assumed to be of the form [1]

$$\eta = \eta_o e^{\gamma P},$$

where γ is 2.22×10^{-2} mm^2/N.

3.7 Experimental Procedure

The wire, after pointing, was passed through the guide, the lubricant container, Christopherson tube and the split die mounted on the dynamometer. The end of the wire was then gripped in the pulling dog which was fixed on the capstan. The dynamometer was supplied with the excitation voltages and the outputs were connected to the recorder. After selecting the required speed, the capstan was rotated by hand to produce initial tension in the wire. The machine was then started. After drawing for some time, stable drawing conditions were obtained when the recorder gave steady readings. All data points were obtained at these steady conditions.

3.8 Experimental Conditions

The experiments were carried out under the following drawing conditions :

Wire :

Material : M.S. annealed wire

Stress-strain equation : $\bar{\sigma} = 260+246.2\ (\bar{e})^{0.63}$ N/mm^2

Initial Diameter : 2.08 mm

Die :

Material : HSS

Half die angle : 3°, 4.5° and 6°

Lubricant :

Light machine oil ; viscosity 65 Centipoise at atmospheric pressure and 28°C.

Drawing speed :

18.09, 31.88, 50.09 and 77.79 m/min.

% Reduction :

14.08 %.

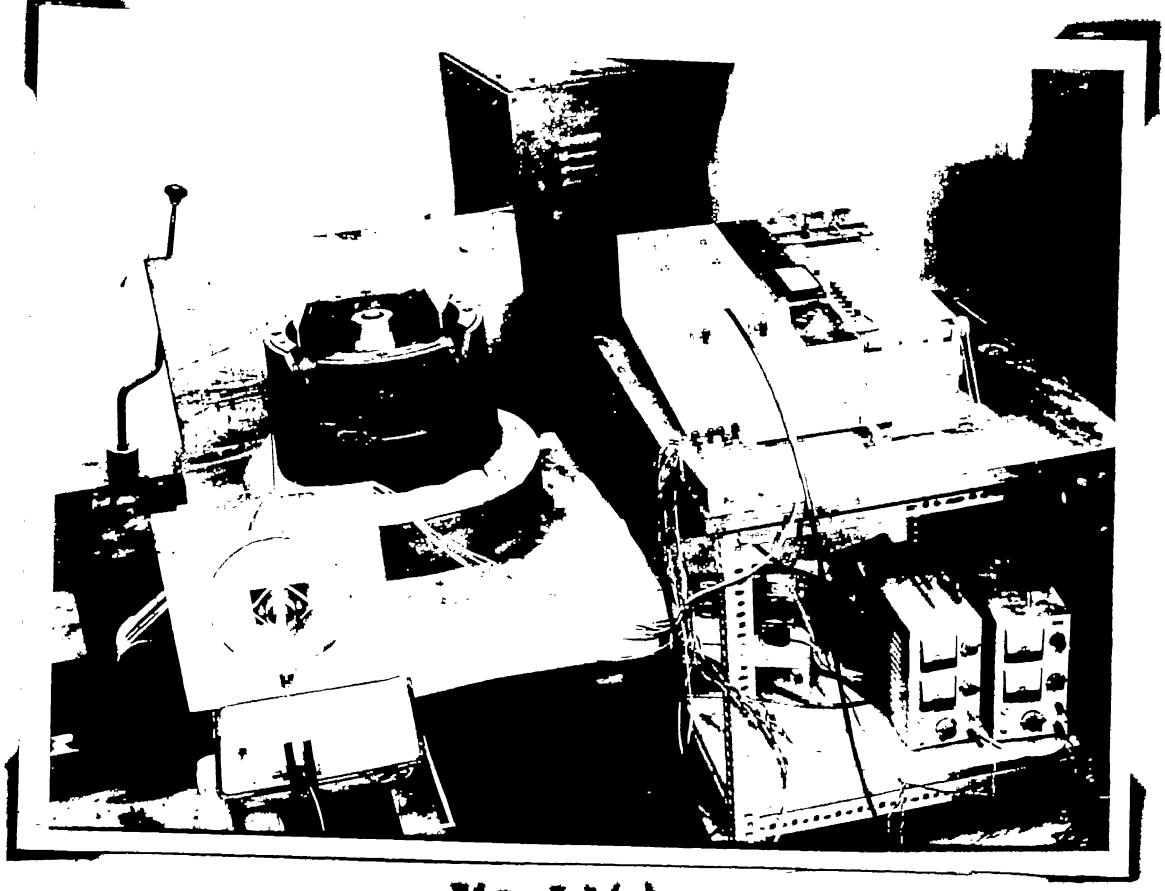

Fig. 3.1(a)

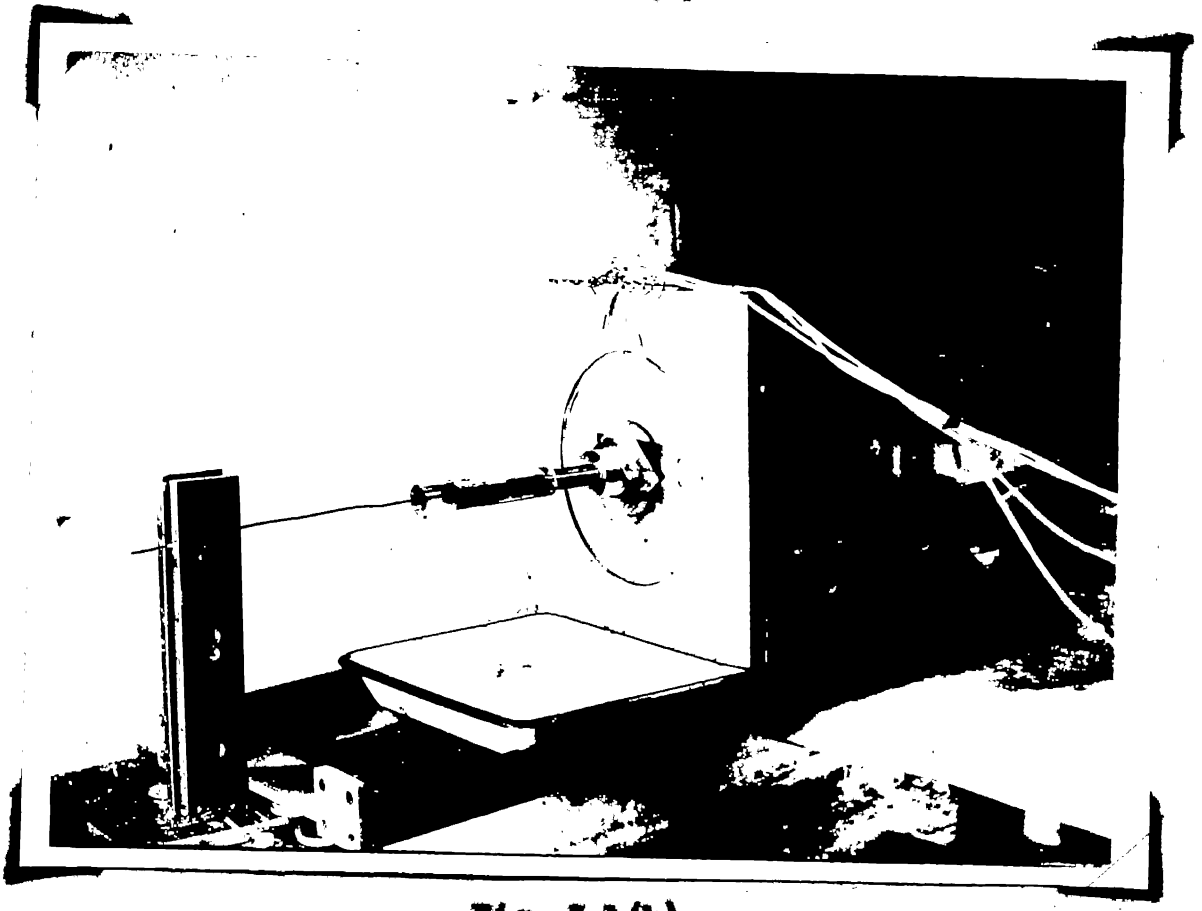

Fig. 3.1(b)

Fig. 3.1 (a) Wire drawing set-up; (b) Lubricant Feed device.

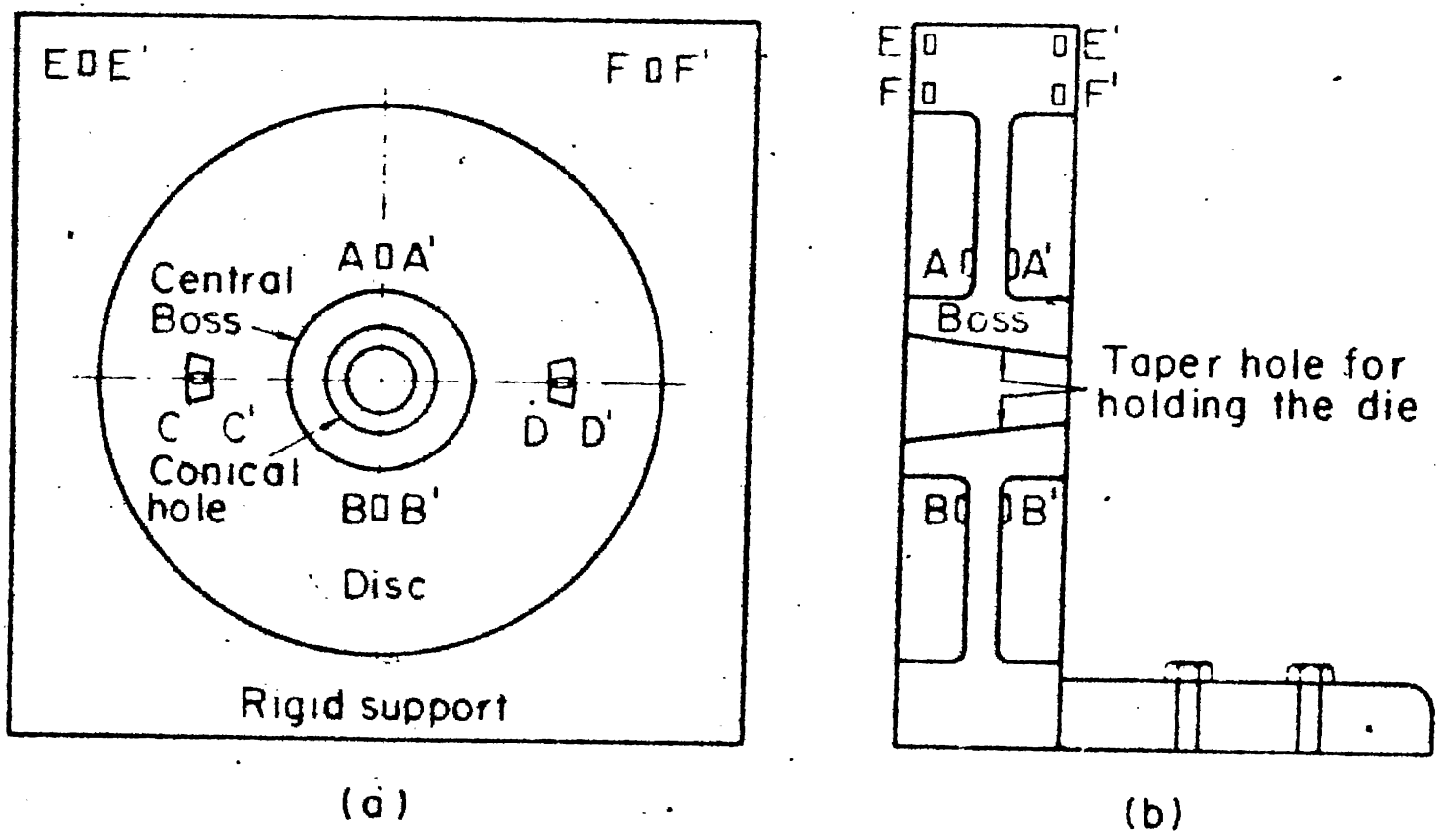

Fig. 32 Details of the disc dynamometer

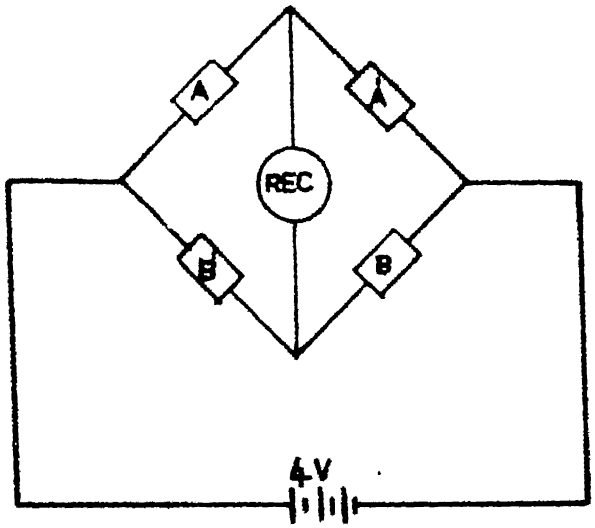

Fig.3.3(a)

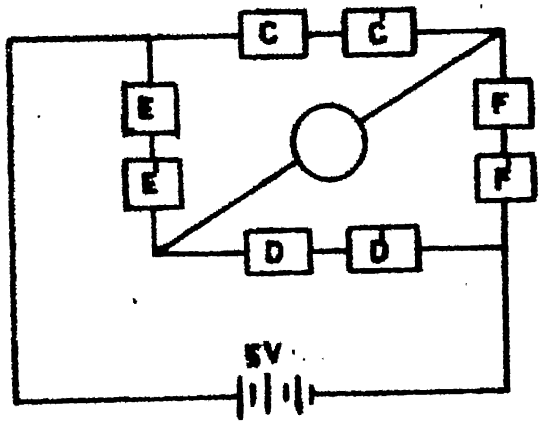

Fig.3.3(b)

Fig.3.3 Bridge circuit for (a) Drawing force, (b) Separating force

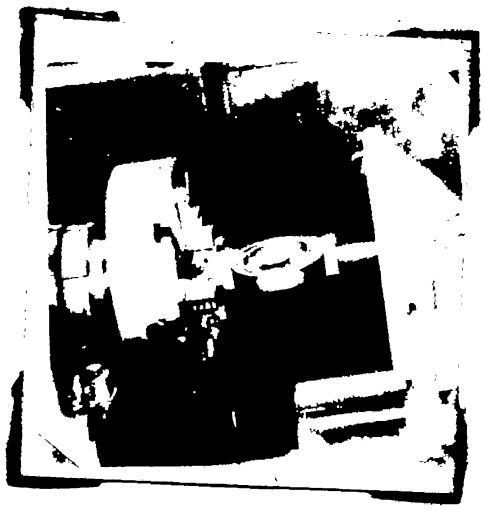

Fig. 3.4 : Dynamometer calibration set-up.

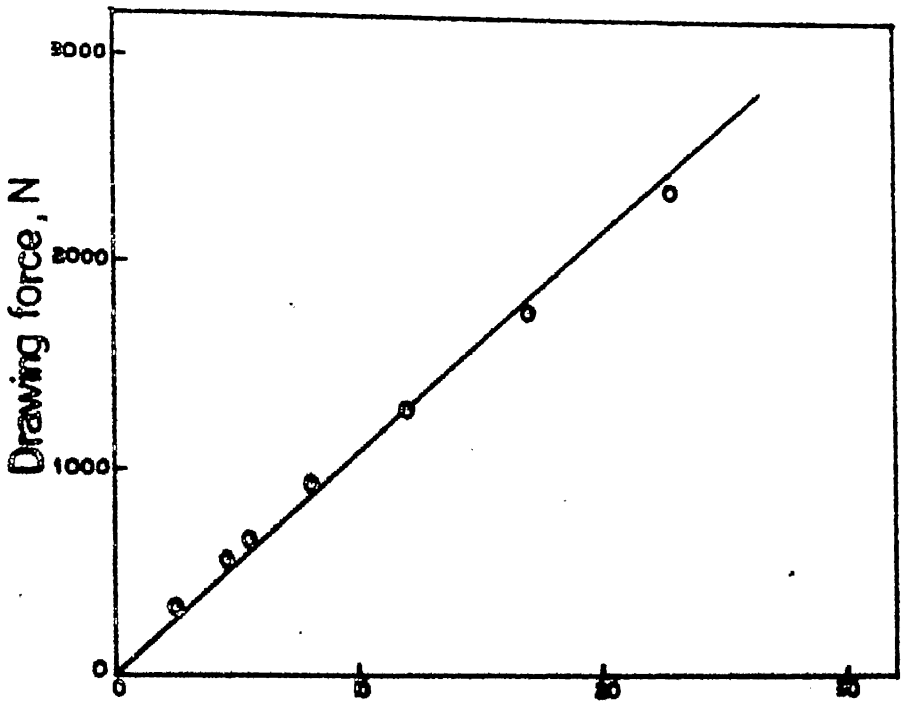

Fig. 3.5(a)

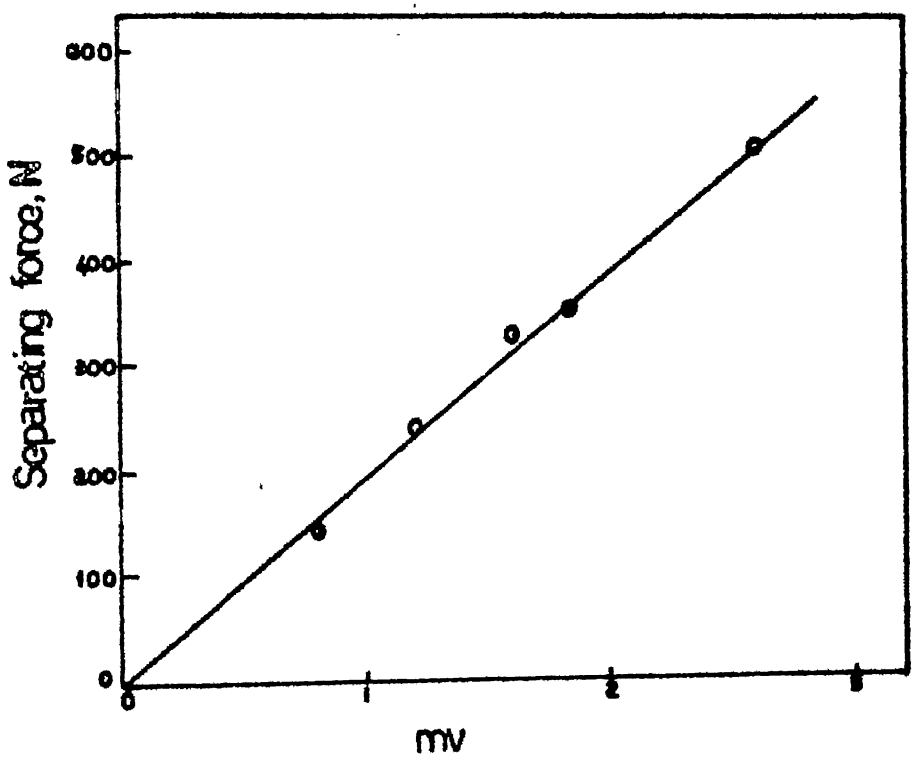

Fig. 3.5(b)

Fig 3.5 Calibration curves: (a) Drawing force; (b) Separating force

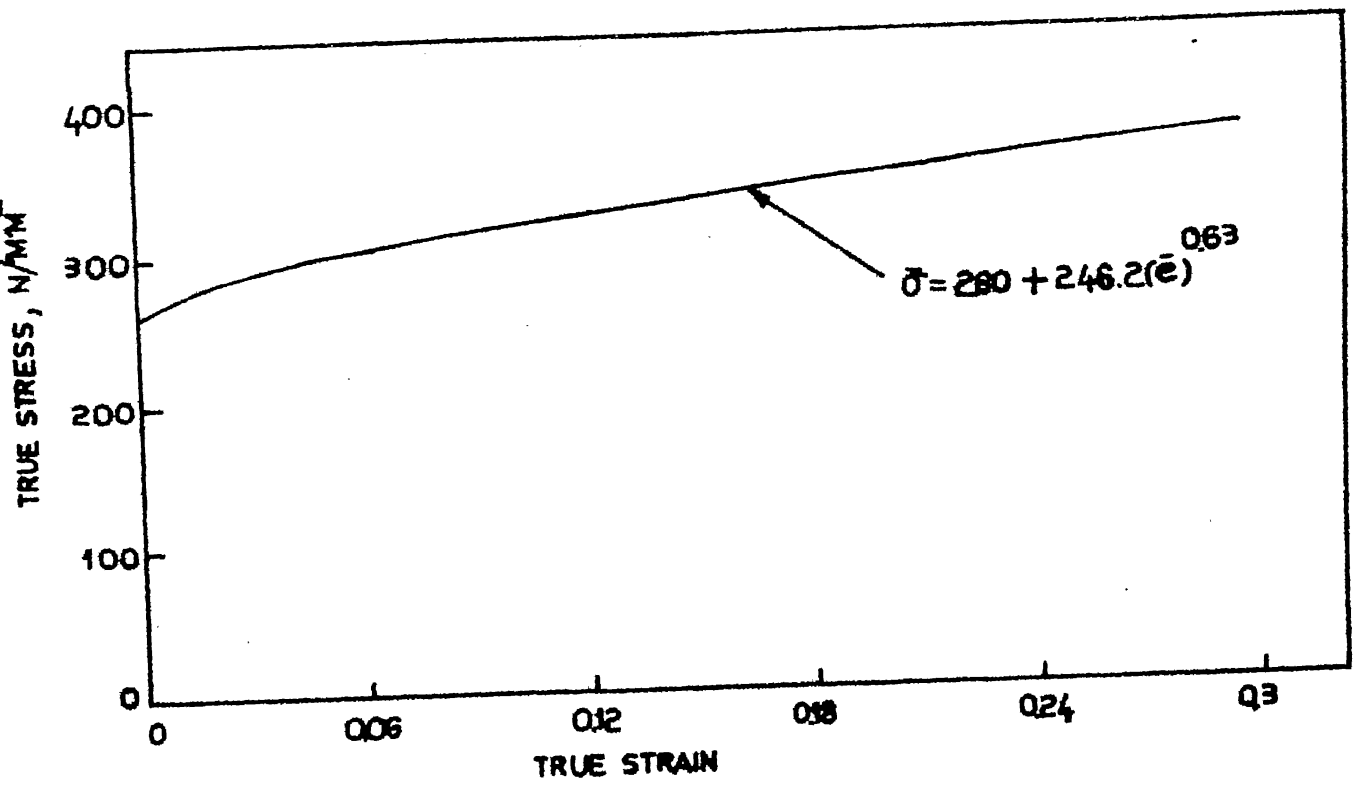

Fig. 3.6 Plastic flow properties of wire material

CHAPTER - IV

RESULTS AND DISCUSSION

4.1 Discussion of Theoretical and Experimental Results

4.1.1 Theoretical Results

An analysis of wire drawing under hydrodynamic lubrication conditions has been presented which differs from earlier attempts [5,7,8] in that the lubricant viscosity has been taken to be pressure dependent and the variation of lubricant film thickness in the deformation zone has been obtained analytically. The analysis is further refined by including the effect of redundant work and strain hardening. The condition for sustained hydrodynamic lubrication has been suggested for wires of different surface roughness. Theoretical results have been obtained for the conditions prescribed in the previous chapter.

Figure 4.1 shows the variation of film thickness within the deformation zone. If the dynamic viscosity of lubricant, speed of drawing, half die angle and pressure at the entry of die are known, film thickness at the entry side can be evaluated from equation (61). If the yield stress of wire material is high and the back tension is small, equation (61) reduces to equation (47) and the film thickness can be evaluated. Equation (61) further indicates that the lubricant film

is thicker when the viscosity is high. The lubricant film thickness also increases with increase in the drawing speed and reduction in the half die angle. That is, if half die angle is small, drawing speed is high and viscosity of lubricant is high, the film thickness is higher and so it can sustain higher load at the die-wire interface. In other words, higher reductions can be achieved or materials exhibiting higher yield stress can be drawn. This agrees with the evidence obtained in the past that the film is thicker when small die angles are employed [12].

Equation (70) gives the criterion for sustained hydrodynamic lubrication. If at any instant, Sommerfeld number (S) is higher than the critical Sommerfeld number (S_c) then only sustained hydrodynamic lubrication can be achieved. In Fig.4.2 S_c is plotted as a function of non-dimensional quantity a. When a is small S_c is very small but it increases exponentially with increase in a. This indicates that for high values of yield stress and low back tension, S_c is high. Fig. 4.3 shows the variation of S_c with another non-dimensional quantity b which indicates an increase in S_c with increase in b. That is, S_c increases with increase in surface roughness of the wire. Therefore, S_c appears to be an important parameter for the study of lubrication effects dueing wire drawing. Further, S should be higher than S_c for sustained hydrodynamic lubrication, which can be achieved by increasing the drawing speed or through use of lubricant of high viscosity and small die angle. For soft wire

materials, S is small and hence, from equation (68), for soft wire materials film is thicker. This also agrees with the results presented earlier [12] that the film is thicker when softer wire materials are used.

Figure 4.4 plots the variation in drawing stress with reduction for various values of yield stress. Here the wire material is assumed to be rigid perfectly plastic. Curves up to 50% reduction have been plotted merely to show the trend of the curve. It is not suggested that the drawing can be carried out at these high reductions. For small reductions, the rate of increase of drawing stress is high but it falls off with further increase in reduction. This is due to decrease in the redundant work with increase in reduction.

Figure 4.5 shows the variation in drawing stress with reduction for a rigid, perfectly plastic material for various value of Sommerfeld number S. It is clear that the drawing stress increases with increase in the value of S. That is, the drawing stress increases with increase in drawing speed and lubricant viscosity. Increase in both of these quantities leads to increased viscous frictional force and hence increased drawing stress.

In Fig. 4.6, the pressure and the stress distribution in the deformation zone are shown for a strain hardening soft copper wire. Pressure distribution obtained is of the same form as observed in the slider bearing [9].

The pressure and the stress distribution for an annealed mild steel wire considering strain hardening effects are plotted in Fig. 4.7. In this case, the pressure at the die surface decreases rapidly in the direction of motion. This can be explained by the fact that, for the conditions used, the lubricant flow is fairly large and the net friction on the wire after leaving the Christopherson's tube is actually reversed, that is, it acts in the direction assisting the motion of the wire. Velocity distribution for this case is shown in Fig.4.8. The lubricant layers near the wire surface are being forced out of the die by the pressure faster than the wire itself. Thus the viscous friction tends to drag the wire forward. This phenomenon was also observed by Christopherson, et al. [1] in their experimental studies.

4.1.2 Experimental Results

The experimental values of drawing and separating forces under the conditions specified in the previous chapter has been tabulated in Table 1.

The lubricant film thickness calculated using equation (61) for $\alpha = 3^{\circ}$, $\eta = 65$ CP and drawing speed of 77.79 m/min is 1.07×10^{-4} mm. For the experimental conditions of the Christopherson and Naylor [1], equation (61) gives the film thickness to be 1.50×10^{-3} mm. Christopherson and Naylor had estimated the film thickness during their tests to be around 10^{-3} mm. Wistreich [2] had also evaluated the value of film thickness from the

measurement of electric resistance at the die-wire interface and suggested that even at moderate drawing speeds the value is of the order of 10^{-3} mm. Equation (61), therefore, appears to predict values of film thickness which are close to the experimentally observed values.

In Fig. 4.9 the drawing and separating forces have been plotted against drawing speed. The surface roughness of drawn mild steel wires is between 1 to 10 micron depending on the total reduction and state of lubricant. For the conditions used in the experiments, the critical Sommerfeld number is about 0.222 for which the drawing speed should be above 720 m/min for sustained hydrodynamic lubrication. But the speed used was quite low and hence would result in unsteady conditions. This was also observed during the experiments as evidencedbby the continual oscillation of the drawing and the separating forces (Fig. 4.10). Based on these observation, and assuming that the microgeometry of the wire surface changes continuously as the deformation proceeds within the die, the mechanism of lubrication can be regarded as a rapid sequence of formation and collapse of hydrodynamic films. That is, the condition prevailing is intermediate between the boundary lubrication and true hydrodynamic lubrication states. Therefore, the conditions prevailing may be termed as 'quasi-hydrodynamic'. Such mechanism of lubrication was also suggested by Wistreich [12]. Lueg et al. [13] also observed continual oscillation of the drawing force.

Ringing wear, a deep and clearly defined annular crater formed at the entry side of die, is the most rapid type of wear observed in wire drawing (Fig. 4.11). In the present experiments no local ringing was observed, but hydrodynamic lubrication was not quite as effective in preventing wear in the sizing portion. The die is practically free from ringing wear due to the fact that the entire bore of the die is continuously under full pressure. In the sizing zone, however, small solid particles in the lubricant can cause wear since the clearance is small.

4.1.3 Comparison of Theoretical and Experimental Results

The critical speed for sustained hydrodynamic lubrication under the experimental conditions and assumed surface roughness is around 720 m/min. As such true hydrodynamic lubrication is not likely to be achieved at the speeds used for the experiments but quasi-hydrodynamic lubrication may be obtained at highest speed used. Hence, for the purpose of comparison, values obtained at the highest speed have been evaluated.

For experimental conditions of $\alpha = 4.5^{\circ}$, drawing speed = 77.79 m/min and $\eta_0 = 65$ centipoise, the analysis for rigid, perfectly plastic material gives the drawing force to be 601.13 N, while the strain hardening analysis gives the drawing and separating forces to be 640.35 N and 301.62 N, respectively.

Corresponding experimental values for the drawing force is 649.91 N and the separating force is 313.92 N. The strain hardening analysis, therefore, predicts values for the drawing and separating forces which are very close to the experimentally observed values.

The experimental data also shows that the decrease in the drawing stress is only marginal (less than 9%) when the speed is increased from 18.09 to 77.79 m/min. Theoretical results also show only a marginal effect of speed on drawing stress (Fig. 4.5).

The surface roughness of the wires used for drawing purposes generally varies between 1 to 10 microns. The theoretical analysis indicates that the sustain hydrodynamic lubrication for such wires of high yield stress is obtained when the drawing speed is quite high much beyond the practical range. In most cases it may not be possible to carry out wire drawing at such high speeds. For e.g., the critical speed for sustained hydrodynamic lubrication is estimated to be beyond 720 m/min for the experimental conditions. The critical speed is also a strong function of the lubricant viscosity and yield stress of the wire material. With highly viscous lubricant and softer wire material it may be possible to achieve the critical speed for true hydrodynamic lubrication. The critical speed for sustained hydrodynamic lubrication is likely to be much lower in such cases. In most cases only quasi-hydrodynamic lubrication

is likely to be achieved. Experiments indicate that even a moderate quasi-hydrodynamic lubrication state can reduce metal to metal contact and improve the die life considerably by decreasing ringing wear.

Table 1 : Experimental Results.

Drawing Speed	Drawing Force, Newton			Separating Force, Newton		
m/min	$\alpha=3^{\circ}$	$\alpha=4.5^{\circ}$	$\alpha=6^{\circ}$	$\alpha=3^{\circ}$	$\alpha=4.5^{\circ}$	$\alpha=6^{\circ}$
18.09	711.22	711.22	748.01	392.4	353.16	343.35
31.88	772.53	698.96	735.75	343.35	240.35	274.68
50.09	698.96	686.7	735.75	294.3	294.3	264.87
77.29	-	649.91	-	-	313.92	-

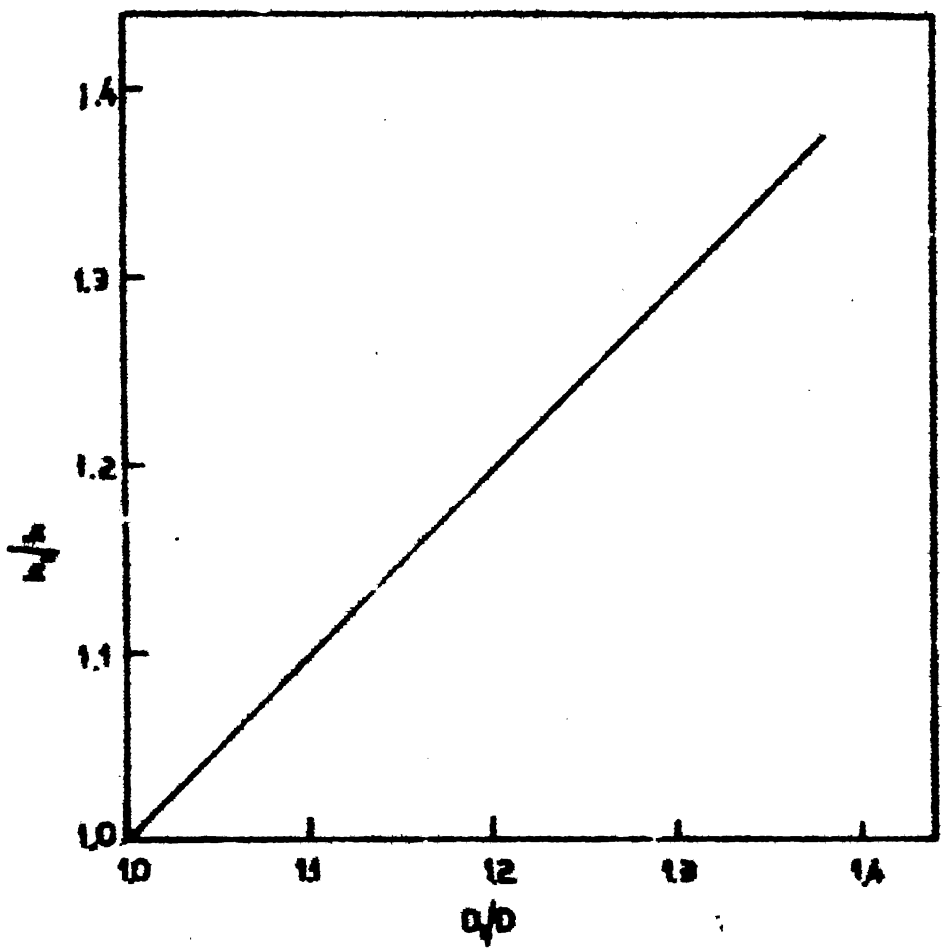

Fig. 4.1 Lubricant film thickness variation within the die

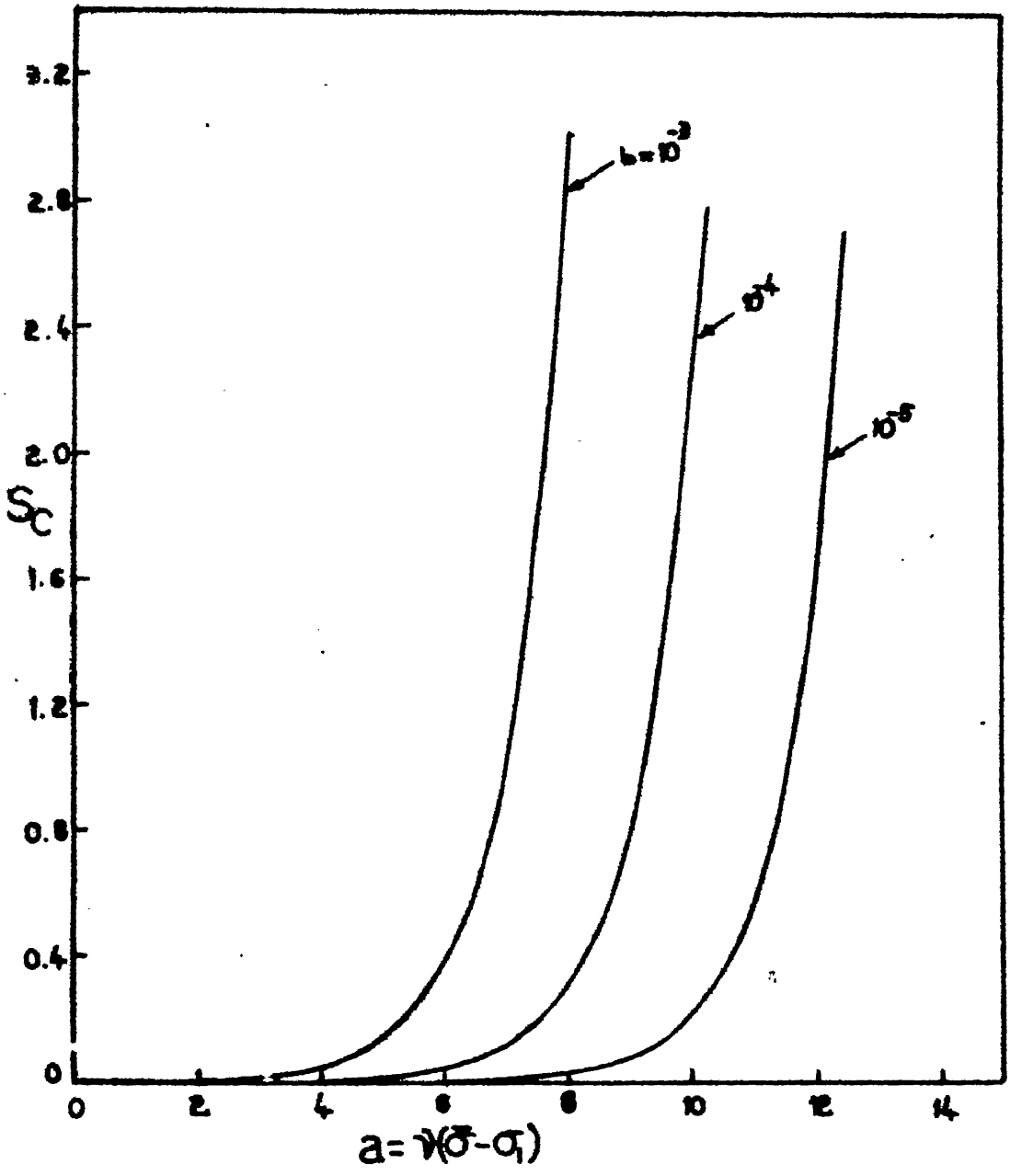

Fig. 4.2 Critical Sommerfeld Number as a function of non-dimensional parameter $\gamma(\bar{\sigma}-\sigma_1)$ for typical non-dimensional values of surface roughness

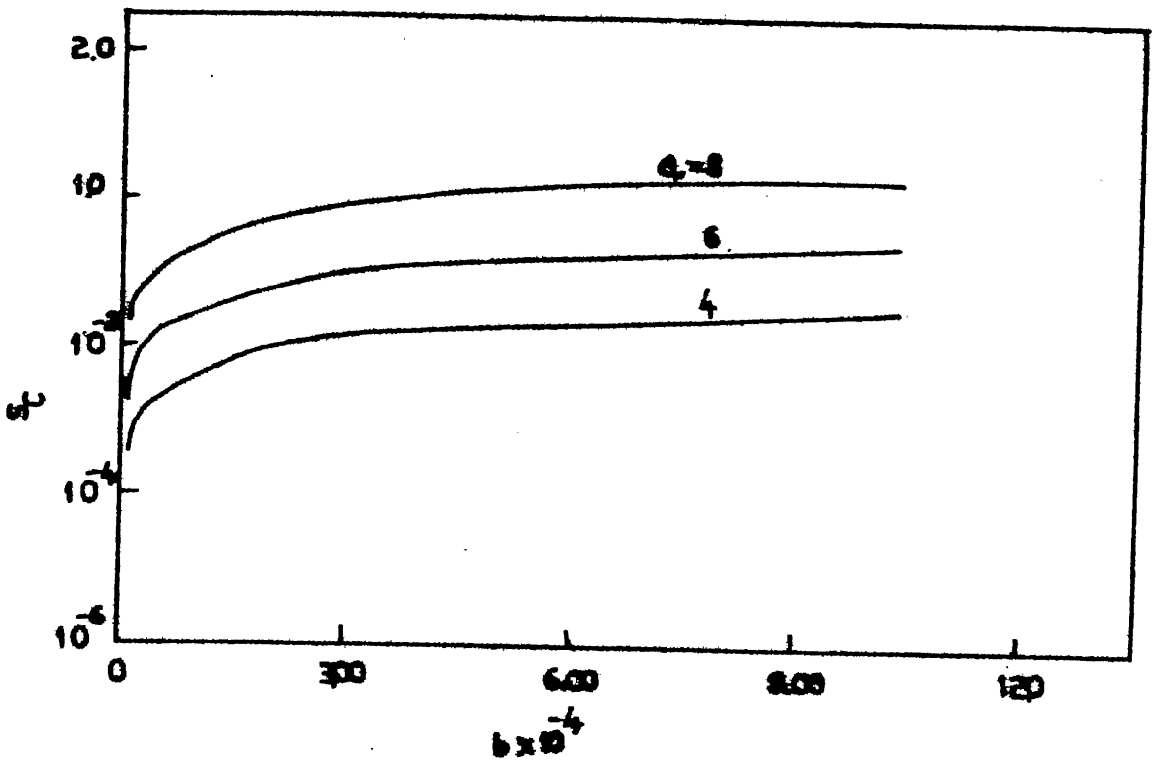

Fig. 4.3 S_c as a function of non-dimensional Surface roughness, b, for typical values of non-dimensional yield stress, a.

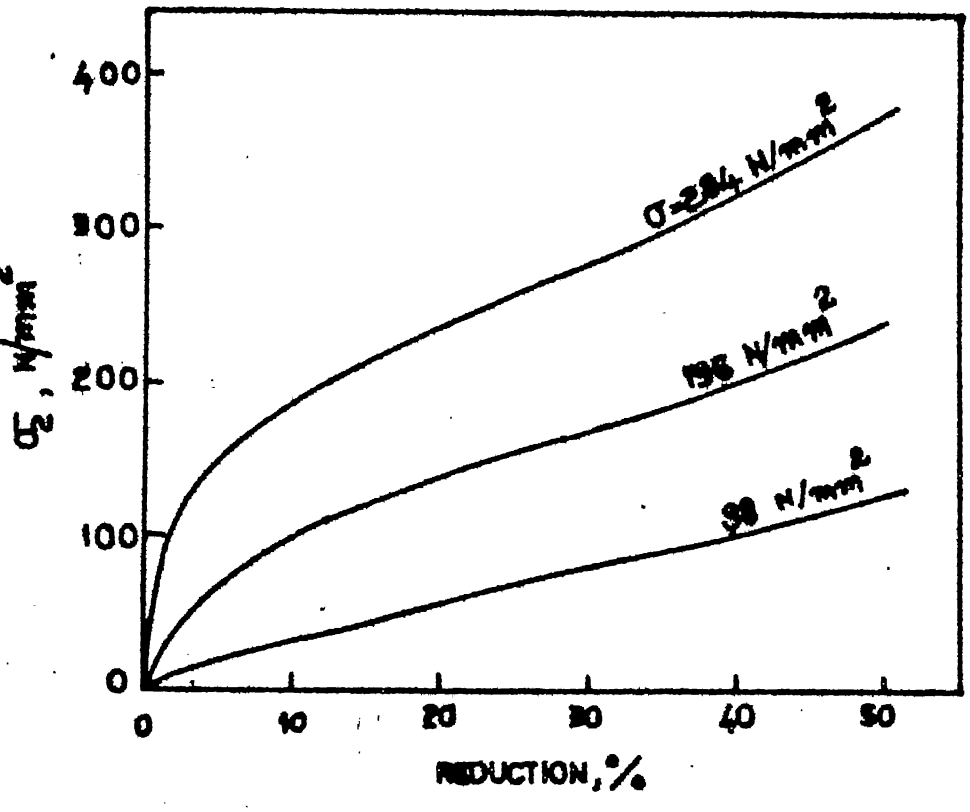

Fig. 4.4 Drawing stress as a function of Reduction for typical values of yield stress (Rigid, perfectly plastic material)

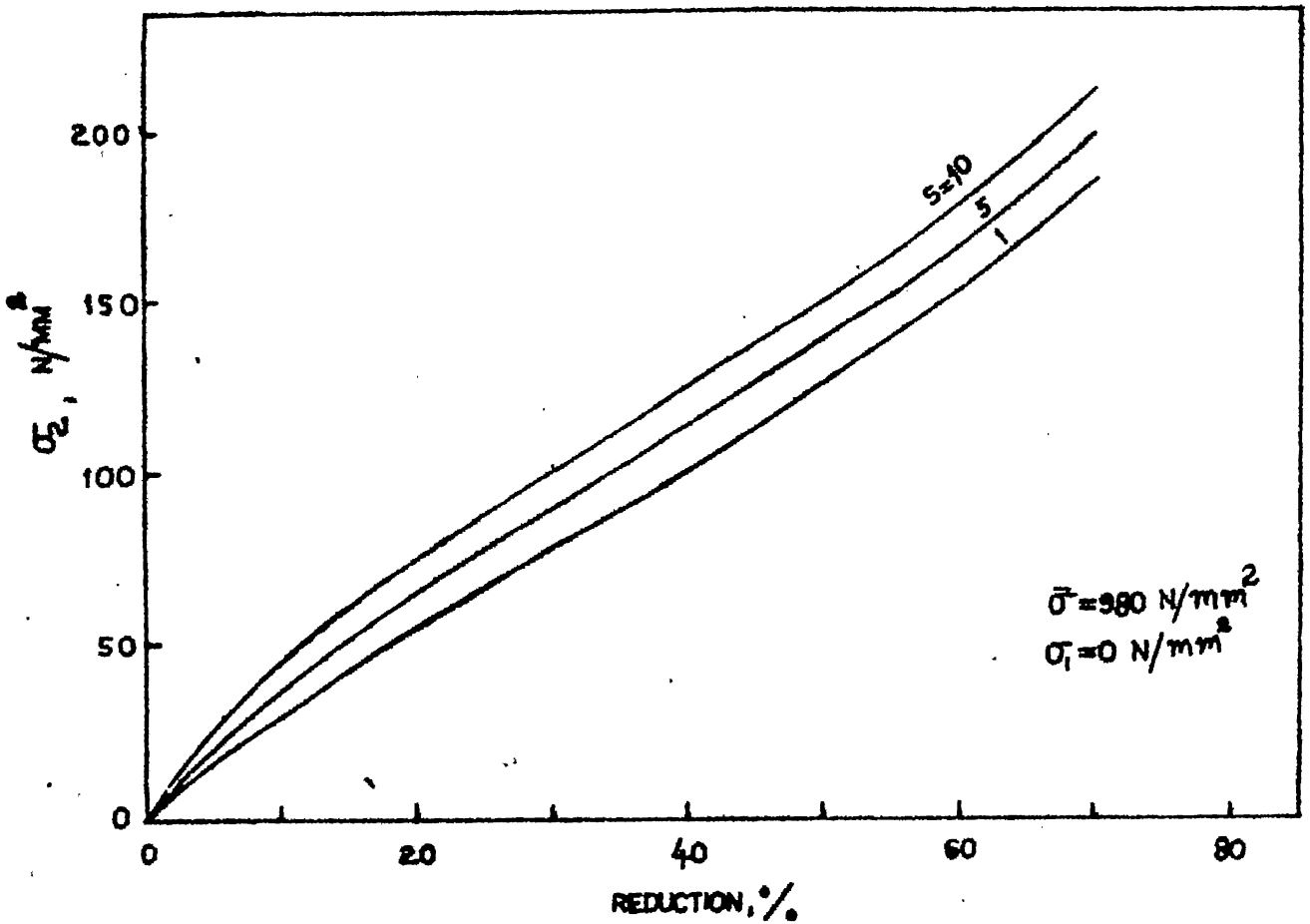

Fig. 45 Drawing stress as a function of Reduction for a rigid, perfectly plastic material

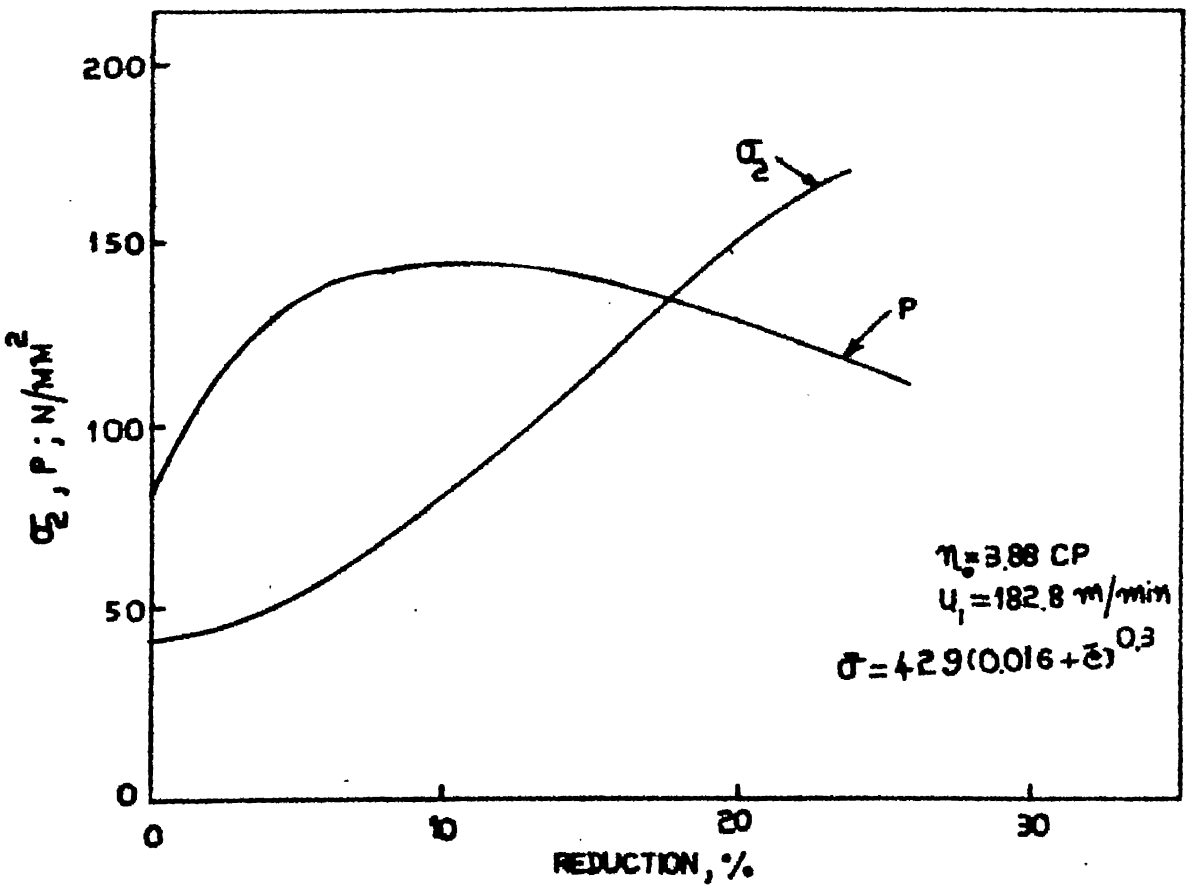

Fig. 4.6 Drawing stress & Pressure as a function of Reduction for strain hardening Soft Copper

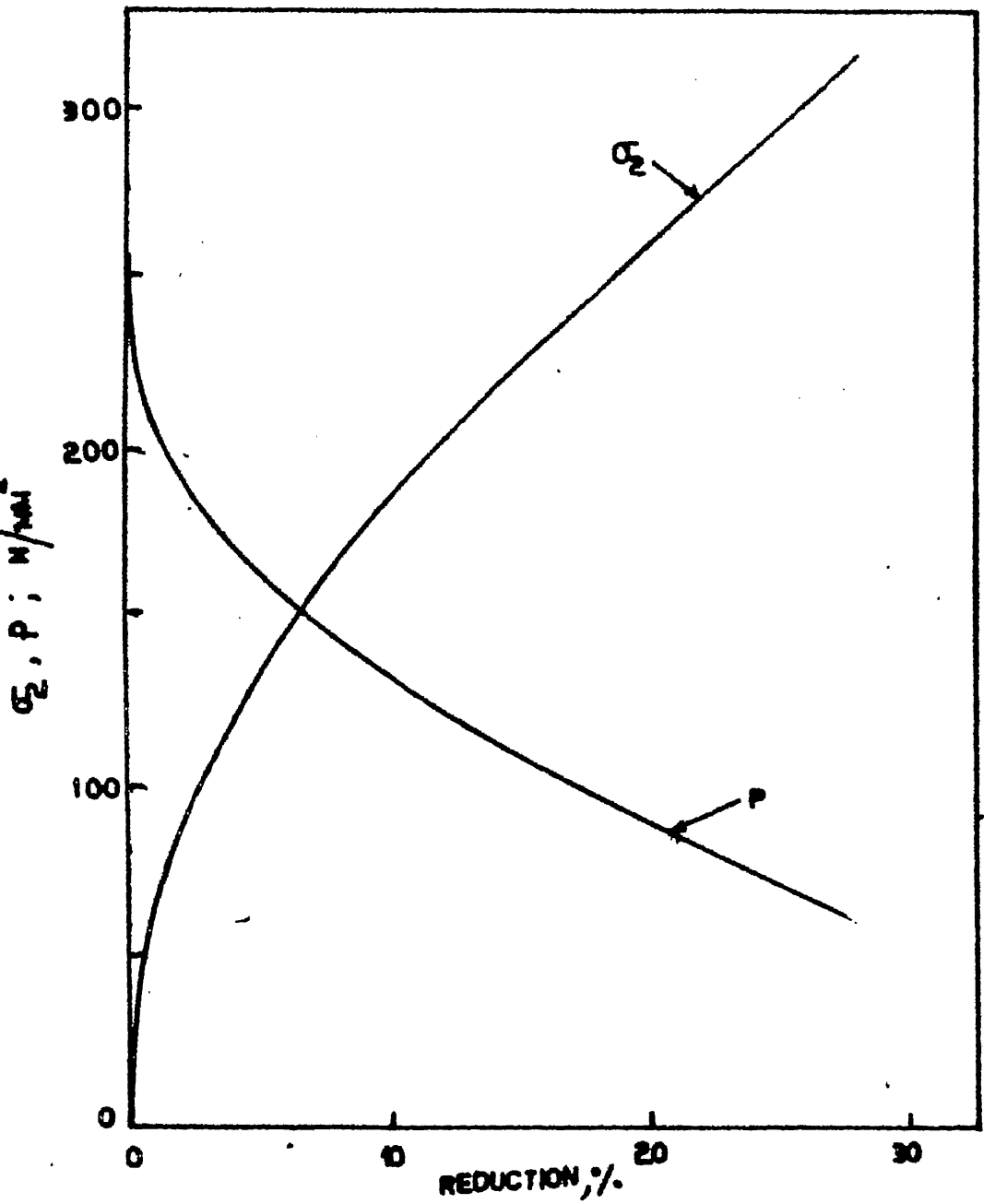

Fig. 4.7 σ_2 & P as a function of Reduction for strain hardening annealed M.S.

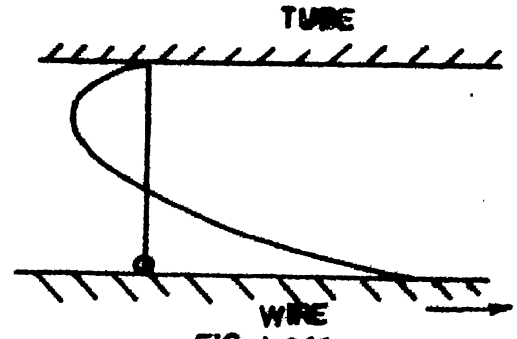

FIG. 4.8 (a)

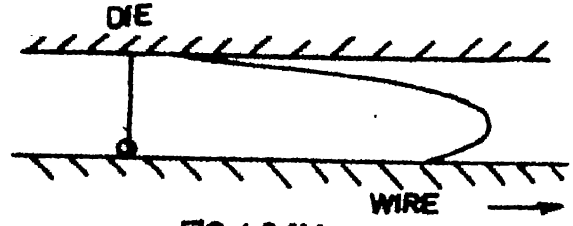

FIG. 4.8 (b)

FIG 4.8 FLOW PATTERN IN: (a) INLET TUBE;
(b) DIE CHANNEL

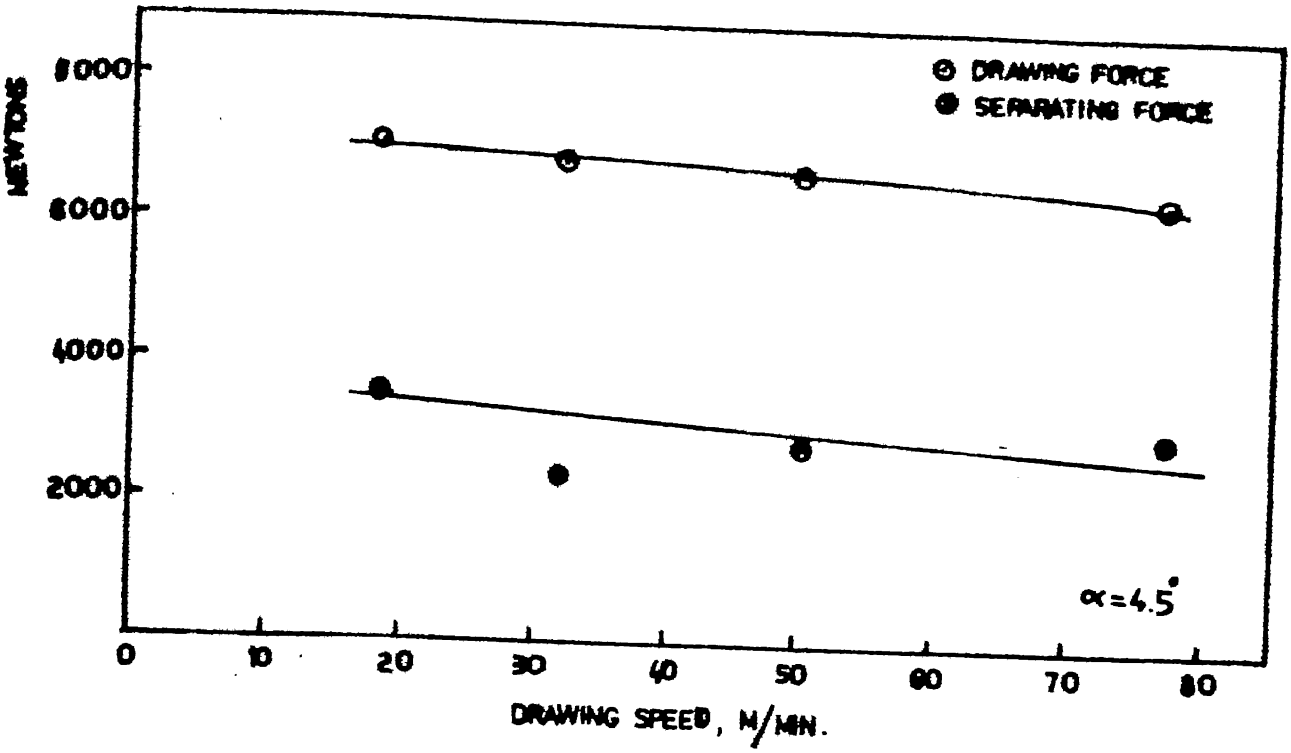

Fig. 4.9 Variation of Drawing and Separating forces with drawing speed

FIG. 4.10(a)

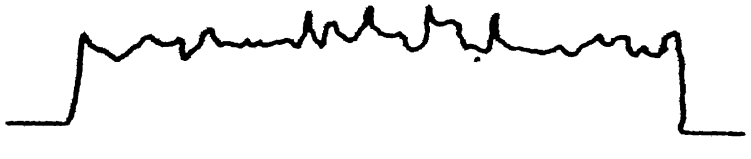

FIG. 4.10(b)

Fig. 4.10 Recorder plot of (a) Separating & (b) Drawing forces

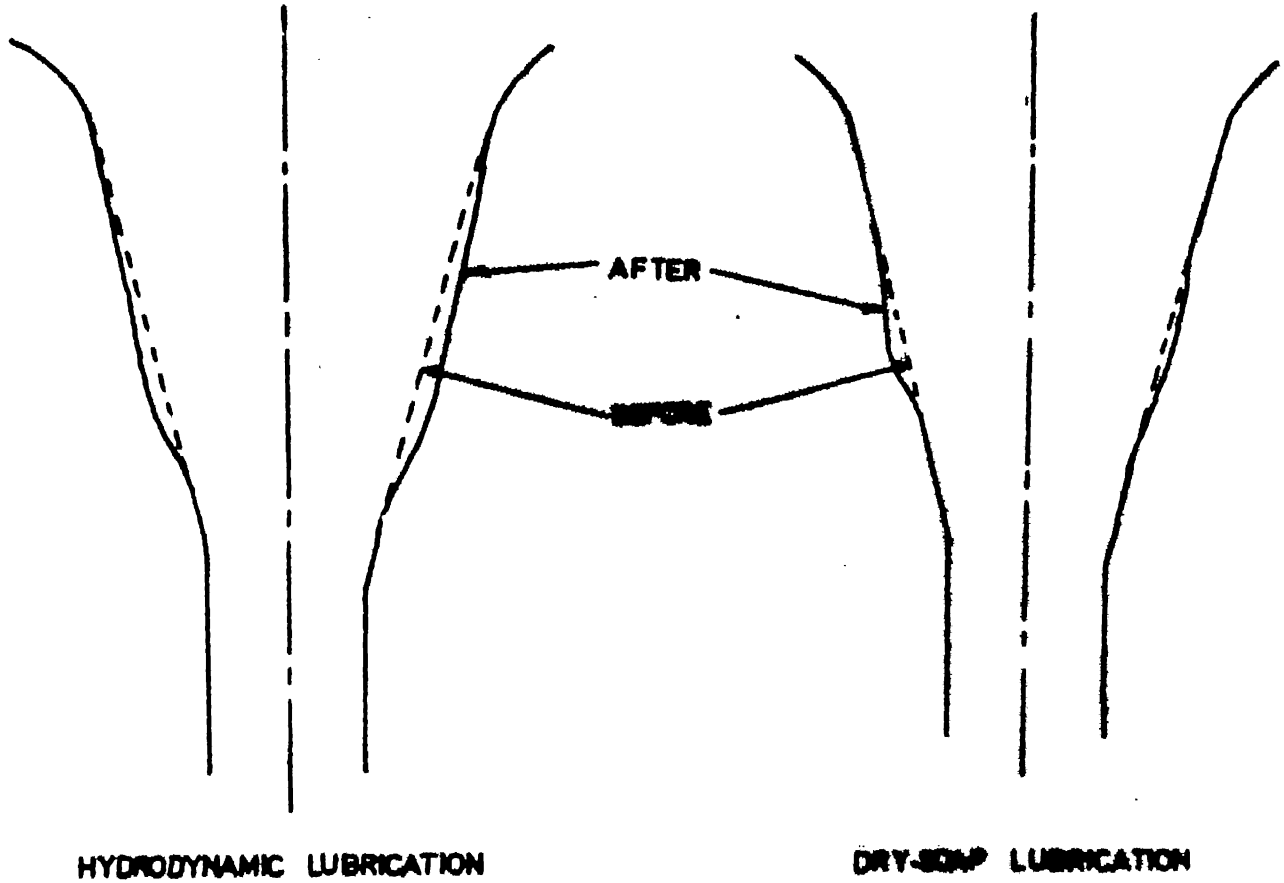

Fig. 4.11 Die Profile Before and After Drawing

CHAPTER - V

CONCLUSIONS

5.1 Conclusion

The theoretical analysis of wire drawing under hydrodynamic lubrication conditions based on equilibrium equation and generalised Reynolds equation for lubricant flow predicts values of film thicknesses which compare well with the published results. It also indicates that the variation of lubricant film thickness in the interface zone is linear. The criterion for sustained hydrodynamic lubrication in terms of critical Sommerfeld number (S_c) appears to be suitable since it provides the value of drawing speed for sustained hydrodynamic lubrication in terms of viscosity of the lubricant and surface roughness of the wire.

Analytical results obtained by idealizing the wire material to be rigid, perfectly plastic shows good agreement with the experimental values of drawing and separating forces. The solution in this case is obtained in close form. Solution for strain hardening material is in very close agreement with the experimental values but the solution needs the application of numerical technique.

The film thickness values evaluated for the experimental data appears to be of the same order as the surface roughness

of the wire. Therefore, only quasi-hydrodynamic lubrication is likely to be achieved. True hydrodynamic lubrication under experimental conditions are likely to be achieved at speeds beyond 700 m/min. Such drawing speeds, however, are not realized in practice. But the absence of ringing wear on the die at the highest experimental speed seems to indicate that achievement of even quasi-hydrodynamic lubrication can enhance the die life considerably.

5.2 Scope for Further Work

The theoretical model presented indicates that the film thickness variation is linear in the interface zone. This needs to be verified experimentally. The value of critical Sommerfeld number under various drawing conditions also needs experimental verification. The theory can also be extended to include the effects of strain rate and temperature.

REFERENCES

1. Christopherson, D.G. and Naylor, H., 'Promotion of fluid lubrication in wire drawing', Proc. Inst. Mech. Engrs., London, Vol. 169, p. 643, 1955.

2. Ranger, A.E. and Wistreich, J.G., J. Inst. Petroleum, Vol. 40, p. 308, 1954.

3. Hillier, M.J., 'A hydrodynamic model of hydrostatic extrusion', Int. Jnl. Prod. Res., Vol. 5, p.171, 1967.

4. Bedi, D.S. and Hillier, M.J., 'A hydrodynamic model for cold strip rolling', Proc. Inst. Mech. Engrs., London, Vol. 182, Part I, p. 153, 1967-68.

5. Bedi, D.S., 'A hydrodynamic model for wire drawing', The Int. Jnl. of Prod. Res., Vol. 6, p. 329, 1968.

6. Avitzur, B. and Grossman, G., 'Hydrodynamic lubrication in rolling of thin strip', Trans. ASME, Vol. 94B, p. 317, 1972.

7. Hashmi, M.S.J., Crampton, R. and Symmons, G.R., 'Effect of strain hardening and strain rate sensitivity of the wire material during drawing under Non-newtonian plasto-hydrodynamic lubrication conditions', Int. Jnl. Mach. Tool Des. Res., Vol. 21, p. 71, 1981.

8. Drupad Ram, 'A hydrodynamic model of wire drawing', M.Tech. Thesis, I.I.T., Kanpur, Aug. 1978.

9. Shaw, M.C. and Macks, F., 'Analysis and lubrication of bearing', McGraw Hill Book Company, Inc., New York, 1949.

10. Tegart, W.J.McG., 'Elements of mechanical metallurgy', The Macmillan Co., New York, 1966.

11. Rowe, G.W., 'An introduction to the principles of metal working', Arnold Press, London.

12. Wistreich, J.G., 'The fundamentals of wire drawing', Metallurgical Reviews, Vol. 3, p. 97, 1958.

13. Lueg, W. and Treptow, K.H., Stahl u. Eisen, Vol. 76, p. 1107, 1956.

APPENDIX-I

Specifications of Wire Drawing Machine

Make : Wire Machinery Manufacturing Corporation Limited, Calcutta.

Model : WM/400/1, Machine No. 1088.

Drawing Speed : 77.75 m/min (Capstan rotating speed).

Capstan circumference : 1.25 m.

Motor : SIEMEN Make, 20 HP, 960 rpm.

Capacity of Machine : Maximum diameter to be drawn

4 mm (Ferrous)

6 mm (Non-ferrous)

Maximum tensile load : 50 kg/mm^2 (M.S.).

APPENDIX-II

Dynamometer Calibration

The dynamometer was calibrated by pushing a tapered plug through the split die mounted on the dynamometer plate. For this situation the equilibrium equation gives the drawing force, F, as

$$F = (A_1 - A_2)\ (1 + \mu \cot\alpha)\ P_m \ . \qquad (a)$$

and the splitting force, F_s, as

$$F_s = P_m \left(\frac{D_1^2 - D_2^2}{4\sin\alpha} \right) (\cos\alpha - \mu \sin\alpha). \qquad (b)$$

Since there is no relative motion (interference fit) the coefficient of friction, μ, in this case is 1. Hence

$$F = (A_1 - A_2)\ (1 + \cot\alpha)\ P_m \qquad (c)$$

and

$$F_s = P_m \left(\frac{D_1^2 - D_2^2}{4\sin\alpha} \right) (\cos\alpha - \sin\alpha) \qquad (d)$$

The force F was applied through a proving ring, hence P_m can be calculated using equation (c). Knowing P_m, F_s can be obtained from equation (d).

APPENDIX-III

Split Die Specifications

Material	:	H.S.S.
Half die angle	:	$3^{\circ}, 4.5^{\circ}, 6^{\circ}$
Inlet diameter	:	2.08 mm
Exit diameter	:	1.928 mm